Design, Synthesis and Characterization of *N*-oxide-containing Heterocycles with In vivo Sterilizing Antitubercular Activity

Guilherme Felipe dos Santos Fernandes,[a,b,c*] Paula Carolina de Souza,[b,g*] Elsa Moreno-Viguri,[c] Mery Santivañez-Veliz,[c] Rocio Paucar,[c] Silvia Pérez-Silanes,[c] Konstantin Chegaev,[d] Stefano Guglielmo,[d] Loretta Lazzarato,[d] Roberta Fruttero,[d] Chung Man Chin,[b] Patricia Bento da Silva,[b] Marlus Chorilli,[b] Mariana Cristina Solcia,[b] Camila Maríngolo Ribeiro,[b] Caio Sander Paiva Silva,[b] Leonardo Biancolino Marino,[b] Priscila Longhin Bosquesi,[b] Debbie M. Hunt,[e] Luiz Pedro S. de Carvalho,[e] Carlos Alberto de Souza Costa,[f] Sang Hyun Cho,[g] Yuehong Wang,[g] Scott Gary Franzblau,[g] Fernando Rogério Pavan,[b#] Jean Leandro dos Santos, [a,b#]

*These authors contributed equally to this work.

[a] São Paulo State University (UNESP), Institute of Chemistry, Araraquara, 14800060, Brazil

[b] São Paulo State University (UNESP), School of Pharmaceutical Sciences, Araraquara, 14800903, Brazil

[c] Universidad de Navarra, Department of Organic and Pharmaceutical Chemistry, Instituto de Salud Tropical, Pamplona, 31008, Spain

[d] Dipartimento di Scienza e Tecnologia del Farmaco, Università degli Studi di Torino, Turin, 10124, Italy

[e] Mycobacterial Metabolism and Antibiotic Research Laboratory, The Francis Crick Institute, 1 Midland Road, London NW1AT, United Kingdom

[f] São Paulo State University (UNESP), School of Odontology, Araraquara, 14801903, Brazil

[g] Institute of Tuberculosis Research, University of Illinois at Chicago, Chicago, 60607, USA.

#Address correspondence to Jean Leandro dos Santos, santosjl@fcfar.unesp.br and Fernando Rogério Pavan, fernandopavan@fcfar.unesp.br.

ABSTRACT

Tuberculosis, caused by the *Mycobacterium tuberculosis* (*Mtb*), is the infectious disease responsible for the highest number of deaths worldwide. Herein, 22 new *N*-oxide-containing compounds were synthesized followed by *in vitro* and *in vivo* evaluation of their antitubercular potential against *Mtb*. Compound **8** was found to be the most promising compound, with MIC_{90} values of 1.10 and 6.62 μM against active and non-replicating *Mtb*, respectively. Additionally, we carried out *in vivo* experiments to confirm the safety and efficacy of compound **8**; the compound was found to be orally bioavailable and highly effective leading to the reduction of the number of *Mtb* to undetected levels in a mouse model of infection. Microarray-based initial studies on the mechanism of action suggest that compound **8** blocks the process of translation. Altogether, these results indicated benzofuroxan derivative **8** to be a promising lead compound for the development of a novel chemical class of antitubercular drugs.

Keywords: *Mycobacterium tuberculosis*, tuberculosis, antitubercular drug, *N*-oxide, furoxan, benzofuroxan.

INTRODUCTION

Mycobacterium tuberculosis (Mtb), the causative agent of tuberculosis (TB) in humans, is considered to be responsible for the highest number of deaths caused by infectious diseases worldwide in 2015. The World Health Organization (WHO) reported 9.6 million new cases and 2 million deaths worldwide in the same year.[1] The high mortality rate of TB has even surpassed the deaths caused by human immunodeficiency virus (HIV). According to an estimation, one-third of the world population is infected with a latent form of TB,[2] where the treatment is often ineffective owing to a lack of drugs with an ability to act in the dormant state of mycobacteria.[3,4]

Furthermore, increased dissemination of multidrug-resistant (MDR), extensively drug-resistant (XDR), and totally drug-resistant (TDR) strains poses a huge challenge to be overcome throughout the world in the fight against TB.[5–8]

For the treatment, the WHO recommends a combination of isoniazid (INH), rifampicin (RMP), ethambutol (EMB), and pyrazinamide (PZA) for six months. In the cases involving resistance, the treatment can be extended up to 28 months and include the use of second-line drugs, such as fluoroquinolones, aminoglycosides, D-cycloserine (DCS), and linezolid (LZD) among others.[9–11] The current treatment suffers from several limitations, including prolonged standard regimen, high rate of treatment discontinuation, adverse effects, toxicity, drug–drug interactions, and a lack of effectiveness against the latent mycobacteria.[2,12–16]

Over the past few years, limited but significant progress in the development of drug candidates against TB has been achieved. After a gap of more than 50 years without new drugs approved for TB, the United States Food and Drug Administration (FDA) approved

bedaquiline (Bdq, SIRTURO,® Janssen; Beerse, Belgium) in 2012 for the treatment of MDR-TB. The literature in the past 5 years has witnessed significant advances in the development of other compounds with potent antitubercular activity.[17–20] In this regard, several drug candidates were moved toward clinical trials, such as sutezolid, posizolid, delamanid, and pretomanid.[21,22] Nevertheless, *Mtb* strains, resistant to the new compounds, have already been reported,[23–25] reinforcing the urgency to develop more potent and a larger number of novel drugs for the treatment of TB.[11]

We have previously reported a series of furoxan derivatives with potent activity against *Mtb*, including MDR strains. Specifically, the compound, (*E*)-4-(4-((2-isonicotinoylhydrazono)methyl)phenoxy)-3-(phenylsulfonyl)-1,2,5-oxadiazole 2-oxide **(Figure 1)** could inhibit 90% growth of *Mtb* H37Rv strain at a concentration of 1 μM. In addition, we characterized that the antitubercular activity of the above-mentioned furoxan derivative was related to its ability to generate nitric oxide (NO) following biotransformation.[26]

Motivated by preliminary promising results obtained with the furoxan derivatives, we designed new heterocyclic analogs containing the N-oxide subunit, including amide-furoxans (series 1), benzofuroxans (series 2), and quinoxaline, 1,4-di-*N*-oxide (QdNO) (series 3, **Figure 1)**. Furoxans, benzofuroxans, and QdNO derivatives represent important scaffolds in medicinal chemistry due to their wide spectrum of biological activities,[27] including antitubercular activity.[28] The antimycobacterial activity of these compounds is attributed to the generation of reactive oxygen species (ROS) following their biotransformation.[29–31] Specifically for quinoxalines, earlier studies have reported that

these compounds lead to increased levels of ROS under hypoxic conditions, which could contribute to interesting properties against latent TB.[32–34]

The ROS play a crucial role in the pathogenesis of TB. Several studies have demonstrated the relationship between the levels of ROS produced by immune cells and the susceptibility of patients to several species of the *Mycobacterium* genus.[35,36] Furthermore, ROS exert many-fold effects during TB. For example, increased ROS levels can lead to an inhibition of *Mtb* growth, damage to cellular components, such as lipids, proteins, and nucleic acids, and activate macrophage-mediated inflammatory activity.[37–40] The high levels of ROS can also induce apoptosis of macrophages (host for tubercle bacilli), thereby preventing the growth and replication of the bacilli.[41] Therefore, the design of new compounds that could act by increasing the levels of ROS and perturbing mycobacterial redox homeostasis seems to be a promising strategy for combating TB.[42–44]

In a continuing effort to develop new drug candidates for the treatment of TB, we herein describe the design, synthesis, and biological activities of a series of heterocyclic compounds containing *N*-oxide as antitubercular compounds.

RESULTS AND DISCUSSION

Chemistry

Twenty-two novel compounds containing the N-oxide subunit were synthesized according to the synthetic methodologies presented in **Schemes 1**, **2,** and **3**.

The amide-furoxan derivatives (**1, 2**) were synthesized according to the previously described methods.[45,46] The furoxan derivative (**2**) was allowed to react with 2-, 3- , or 4-hydroxybenzaldehyde in dichloromethane medium, using 1,8-diazabicyclo[5.4.0]undec-

7-ene (DBU) as the base, leading to the formation of the furoxan derivatives containing an aldehyde group (**3a**–**c**).[47] Then, a condensation reaction of the aldehyde derivatives with isonicotinohydrazide was performed in ethanolic medium catalyzed by an acid to generate the hybrid furoxan derivatives (**4a**–**c**, **Scheme 1)**.

The benzofuroxan derivative containing an aldehyde group (**7**) was obtained according to a previously reported methodology.[48] The compound was allowed to react with different aromatic hydrazides through the same condensation reaction described above leading to the formation of benzofuroxan derivatives (**8**–**17**, **Scheme 2)**. The ^{1}H and ^{13}C nuclear magnetic resonance (NMR) spectra of these compounds displayed protons and carbon signals from the benzofuroxan nucleus as broad peaks, indicating a benzofuroxan tautomerism.[27,31]

The dioxolan-benzofuroxan derivative (**18**) was obtained from the reaction between compound (**7**) and ethylene glycol.[49] The quinoxaline derivatives were obtained through a variation of the Beirut reaction,[50–52] wherein the dioxolan–benzofuroxan derivative (**18**) reacted with the appropriate nitrile derivatives in dichloromethane medium. Potassium carbonate (K_2CO_3) was utilized as a catalyst[53] leading to the generation of quinoxaline derivatives (**19**–**26**). Compound (**28**) was synthesized from quinoxaline (**19**), which was submitted to a cyclic acetal hydrolysis followed by its reaction with isonicotinohydrazide through a condensation reaction **(Scheme 3)**.[54]

All compounds were characterized by elemental analysis, infrared (IR) spectroscopy, mass spectrometry, and ^{1}H and ^{13}C NMR. Furthermore, all compounds were analyzed by high-pressure liquid chromatography (HPLC) and their purity was confirmed to be

superior to 98.5%. Experimental logP values and melting points were determined for the final compounds.

Biological studies

The antitubercular activity of compounds containing *N*-oxide (**4a**–**c**, **8**–**17**, **19**–**26,** and **28**) was performed using *Mtb* H_{37}Rv ATCC 27294 strain. The resazurin microtiter assay (REMA) was employed as described previously.[26,55] The results were expressed as minimum inhibitory concentration (MIC_{90}) and compounds showing MIC_{90} values below 10 μM were selected for further characterization. The potential cytotoxicity was evaluated using human lung fibroblast, MRC–5 according to a previously reported methodology[26,56] and the results were expressed as IC_{50} values. The selectivity index (SI) of the tested compounds was calculated through the ratio between IC_{50} and MIC_{90}. The compounds that reported SI ≥ 10 were considered promising for further studies according to the cutoff value established.[56,57] Potential anaerobic activity of the best compounds was evaluated using the method described by Cho *et al.*, 2007.[58]

The analysis of the spectrum of biological activity of the compounds was performed through determination of MIC_{90} values against *Escherichia coli* (ATCC 25922) and *Staphylococcus aureus* (ATCC 29213) by measuring the optical density (OD) at 570 nm (OD_{570}) after 16 h and against *Candida albicans* (ATCC 10231) at OD_{570} nm after 48 h.

The compounds were also tested against *Mtb* H_{37}Rv isogenic strains monoresistant to RMP (ATCC 35838); INH (ATCC 35822); streptomycin (SM, ATCC 35820); capreomycin (CAP), moxifloxacin (MOX), and BDQ (strains from the University of Illinois at Chicago-Institute for Tuberculosis Research) by microdilution technique

multiple antigen blot assay (MABA).[59] Following this step, we selected the best compound (compound **8**) for further studies.

Due to the ability of *Mtb* to survive inside the macrophages, we decided to investigate whether compound **8** could inhibit the growth of *Mtb* H37Rv strain in J774A.1 macrophage cell line. Furthermore, time-kill experiments were performed for up to 15 days to evaluate the bactericidal profile of compound **8**.

Some earlier reports[60,61] indicated that the growth of mycobacteria can be affected by the presence of ions, nutrients, and pH of the medium. With this regard, different conditions of culture medium were analyzed by MABA. These included (a) adjusting the culture medium to pH 6.0; (b) including 4% bovine serum albumin (BSA); and (c) the supplementation of 10% fetal bovine serum (FBS). The slightly acidic pH (pH 6.0) was selected as the pH compatible to the growth of *Mtb* and corresponding to the time of fusion of *Mtb*-containing phagosomes with lysosomes. One of the physiological functions of albumin (synthesized in the liver) is to transport of poorly soluble molecules of both endogenous and exogenous origin.[62] Albumin binding constitutes an essential pharmacological parameter that affects the mechanism of action of antibiotics in humans.[63] We utilized FBS, as it serves as a growth factor for mammalian cells and might interfere with the antitubercular action of some compounds.

Preliminary ADMET (abbreviation for absorption, distribution, metabolism, and excretion) studies were performed for compound **8** using the following *in vitro* assays: chemical stability assay, plasma protein binding assay, caco–2 permeability assay, cytochrome P450 inhibition assay, and hepG2 cytotoxicity. Additionally, we

characterized the mutagenicity of compound **8** through the micronucleus assay using the mouse peripheral blood reticulocytes.

To ensure a greater stability and improved solubility, compound **8** was evaluated in an *in vivo* assay using a pharmaceutical formulation. The nanostructured lipid system (ME) was synthesized as described by our group previously,[64] with the following composition: 10% oil phase (cholesterol), 10% surfactant (a mixture of soy phosphatidylcholine, sodium oleate, and Eumulgin® HRE 40 [polyoxyl 40 castor oil-hydrogenated]; 3:6:8), and 80% aqueous phase (phosphate buffer, pH 7.4). The compounds studied were incorporated at the desired concentration for the *in vivo* experiments by mass solubilization at the respective volume and sonicated for 3 min in the batch mode at 15% amplitude. The ME containing compound **8** was analyzed for tolerability and oral bioavailability following the treatment of female BALB/C mice infected with *Mtb*.

Microarrays have been used to define successfully the mechanism of action (MOA) of antitubercular compounds.[65] Therefore, a microarray analysis was performed to obtain an unbiased view of the MOA of compound **8.**

In Vitro Antimycobacterial Activity

The ability of *Mtb* to remain dormant serves as the predominant factor that contributes to precluding sterilization with antibiotic therapy and promotes the development of antibiotic resistance.[66,67] Therefore, an ideal antitubercular drug should (i) reduce the duration of treatment; (ii) be active against resistant strains; (iii) not interfere with other TB drugs and antiretrovirals; and (iv) be active against “dormant” bacilli.[10]

Recently, our research group has identified the compound, (*E*)-4-(4-((2-isonicotinoylhydrazono)methyl)phenoxy)-3-(phenylsulfonyl)-1,2,5-oxadiazole 2-oxide as a promising antitubercular drug candidate.[26] To optimize its antimycobacterial activity, we designed novel heterocyclic compounds containing *N*-oxide analogs of the parent compound, which comprised the following heterocyclic moieties: amide–furoxan (series 1, **4a**–**c**), benzofuroxan (series 2, **8**–**17**), and quinoxaline 1,4-di-*N*-oxide (series 3, **19**–**26**, **28**). The amide–furoxan derivatives (**4a**–**c**) were selected to evaluate whether the replacement of the phenylsulfonyl group from the parent compound by an amide group would increase the antitubercular activity and/or decrease the cytotoxicity. The three amide–furoxan regioisomers (**4a**–**c**) displayed an improved antitubercular activity than the parent compound.[26] The compounds from series 1 exhibited MIC_{90} values around 0.4 μM against actively growing *Mtb* H_{37}Rv strain **(Table 1)**.

The benzofuroxan moiety (series 2, **8**–**17**) was selected due to its possible ability to generate ROS after its metabolism.[30] The structural design of the series under the study was based on the isosteric replacement of substituents attached at the *para* position on the phenyl ring. These included hydrogen, nitro, *tert*-butyl, amino, and hydroxyl groups. Furthermore, we evaluated the substitution of the phenyl ring by a pyridine ring owing to the presence of heterocyclic pyridine ring in the structure of several antituberculosis drugs and bioactive compounds, such as INH, BDQ, and ethionamide.[68] As expected, the replacement of the phenyl ring of compound **9** by a pyridine ring in compound **8** led to a seven-fold increase in the antituberculosis activity (MIC_{90} = 1.1 μM, **Table 1)**.

Among the benzofuroxan series, our group could identify the compound, (*E*)-6-((2-isonicotinoylhydrazono)methyl)benzo[c][1,2,5]oxadiazole 1-oxide (**8**) as the lead

benzofuroxan derivative with MIC_{90} values of 1.1 and 6.6 μM for actively growing and dormant *Mtb*, respectively. The observed nearly equimolar effects against replicating and non-replicating *Mtb* attributed to the small difference in MIC_{90} values is considered as an attractive characteristic. Such differences are rarely observed but highly desired and beneficial.

Moreover, our data revealed that the presence of bulky groups, such as *tert*-butyl (**10**, MIC_{90} = 3.9 μM) and electron-withdrawing groups, such as nitro (**11**, MIC_{90} = 5.3 μM), led to an improvement in antituberculosis activity of the analyzed compounds. Compound **9**, un-substituted phenyl, presented a MIC_{90} value of 8.3 μM, while the hydroxyl regioisomers (**12**–**14**) presented MIC_{90} values greater than 62 μM. Amino derivatives (**15**–**17**) also exhibited a reduction in the antitubercular activity in comparison to the non-substituted compounds **9**; however, these compounds reported MIC_{90} values (12.3– 27.9 μM) lower than those containing a hydroxyl substitution **(Table 1)**.

With respect to the quinoxaline, 1,4-di-*N*-oxide series, we evaluated the influence of electron-withdrawing and electron-donating groups on the phenyl ring for its antitubercular activity. We also performed an isosteric substitution of the phenyl ring by furan (**25**) and thiophen (**26**) moieties. For quinoxaline-phenyl derivatives (**19**–**24**), the MIC_{90} values ranged from 12.0 to 30.8 μM, implying a contribution of the presence of substitution at the *para* position of the phenyl ring to the antituberculosis activity. Since compound **19** was devoid of any substituents, it displayed a lower potency among the phenyl quinoxaline derivatives with MIC_{90} = 30.8 μM. On the other hand, compound **22**, with a methoxyl group in the *para* position, displayed the lowest MIC_{90} value among the

phenyl quinoxaline series. Nevertheless, we could not observe a clear and accurate structure–activity relationship regarding the electronic properties of the substituents.

For compounds **25** and **26**, the isosteric replacement of the phenyl group by a furan or thiophen ring led to a significant increase in the antitubercular activity. Compounds **25** and **26** exhibited MIC_{90} values of 5.2 and 12.1 μM, respectively. Furthermore, we synthesized a quinoxaline derivative containing an *N*-acylhydrazone subunit (**28**); the antitubercular activity of this compound decreased in comparison to the previous quinoxalines exhibiting MIC_{90} value of 39.7 μM.

Further *in Vitro* Biological Profiling of Selected Compounds

We evaluated the cytotoxicity of the final compounds against MRC–5 cell lines. This cell line is derived from healthy human lung fibroblasts and is widely utilized for the phenotypic screening of antitubercular drugs.[69–71]

The data obtained in the cytotoxicity studies of the amide–furoxan series (**4a**–**c**) indicated a high selectivity of these compounds against *Mtb*. All three regioisomers exhibited high IC_{50} values (>854.0 μM), thereby leading to high SI values, which ranged from 2,033 to 3,205 **(Table 1)**.

Regarding the cytotoxicity studies of the benzofuroxan series, we observed IC_{50} values ranging from 25 to 841 μM in MRC–5 cell lines. The most active benzofuroxan derivative (**8**) presented an IC_{50} value of 519 μM; however, the compound **17** was found to be less cytotoxic among the benzofuroxan series with an IC_{50} value of 841 μM. Compounds **11** to **14** did not display promising antitubercular activity (MIC_{90} > 62 μM) and consequently were excluded from the cytotoxicity studies. Rather, compound **8** was

selected for further experiments, as it possessed the highest potency against *Mtb* and the lowest cytotoxicity.

Compounds from quinoxaline series were significantly more cytotoxic in MRC–5 cells with their IC_{50} values ranging from 13 to 67 μM, thereby resulting in low SI (<6.8) values and making them less attractive candidates as antitubercular agents.[56]

The data obtained from MIC_{90} in different conditions (**Table 2)** depicted no significant differences between MIC_{90} under normal and others conditions. These conditions included (a) adjusting the pH of the culture medium to 6.0; (b) including 4% BSA; and (c) supplementation of 10% FBS.

Antimicrobials are classified as containing narrow, intermediate, or broad spectrum of activity. Tuberculosis is a chronic infection, the treatment of which requires a drug with narrow spectrum, such as INH. All amide–furoxan and benzofuroxan (**8, 11, 14,** and **17**) derivatives were checked against *S. aureus*, *E. coli*, and *C. albicans*. No antimicrobial activity was detected up to a maximum concentration of 200 μM.

In terms of cross-resistance, compound **8** displayed equipotent activity (<two-fold change in MIC_{90}) against all drug-sensitive and monoresistant strains of *Mtb* tested, suggesting a novel MOC or inhibition of a shared target distinct binding site by the compound **(Table 3)**. In contrast, amide–furoxan series (**4a**–**c**) was inactive against half of the monoresistant strains tested and therefore was not selected for further studies.

We utilized J774A.1, a macrophage cell line, to study the intracellular inhibition of *Mtb* using the drugs under analysis. Our group observed that compound **8** exhibited a high intracellular inhibition at all concentrations tested (around 90%). However, similar to RMP, we could not verify the dose-dependent inhibition at different concentrations

(Figure 2). In time-kill kinetic experiments, compound **8** was observed to be bactericidal with an early bactericidal effect. Noteworthy, compound **8** could sterilize the cultures after 48 h of exposure (about of 6.7 log10, **Figure 3)**.

Preliminary ADMT Studies of Compound 8

On the basis of the promising biological results described above for compound **8**, we conducted stability and ADMT studies to assess its drug-like properties, such as absorption, distribution, metabolism, and excretion. To analyze the chemical stability of the compound, we conducted an *in vitro* assay under two pH conditions (5.5 and 7.4) to mimic the environment of a macrophage phagolysosome (pH 4.5–6.2)[72,73] and the neutral plasma (pH 7.4). At pH 5.5 and 7.4, the compound **8** exhibited a good stability **(Figure 4)**; however, a reduction of 20% was detected at both pH values after 10 h. Interestingly, the concentration of compound **8** increased to 67 and 75% at pH 5.5 and 7.4, respectively, after 24 h. The degradation rates of compound **8** were calculated by HPLC-UV; however, we did not characterize the degradation products. These results indicated that the compound **8** exhibited a high stability in the physiological pH range in the target areas of bacteria, namely, blood and phagolysosome.

The *in vitro* ADMT properties for compound **8** are listed in **Table 4**. The benzofuroxan derivative reported 46.5% unbound fraction when an *in vitro* plasma protein binding assay was conducted. The findings of the study with compound **8** on the inhibition of cytochrome P450 isoforms depicted no potential for inhibition, presenting IC_{50} values greater than 15.0 μM in all isoforms tested. The studies in the Caco–2 cell line demonstrated a good permeability profile. The cytotoxicity study conducted in HepG2

cells reported an IC_{50} of 16.0 μM and an SI of 14.5. We also performed the micronucleus assay using mouse peripheral blood reticulocytes for compound **8** to evaluate its intrinsic mutagenic activity. The results indicated that compound **8** was not genotoxic at all concentrations tested (**Figure 5**).

Tolerability, Oral Bioavailability, and Efficacy of Compound 8 in Mice

In vivo oral bioavailability, toxicology, infection, and treatment studies were performed to ensure the safety and efficacy of compound **8**.

For toxicology studies, the mice were monitored daily for 10 days, receiving one daily oral dose (by gavage, 200 mg/kg body weight), and the behavior parameters (hippocratic screening) were evaluated. No significant variation in the behavior of mice was observed during the period of 10 days. Changes in the weight of organs (heart, lungs, spleen, kidneys, and liver) were evaluated using analysis of variance (ANOVA) and Dunnett's test, establishing a p-value < 0.05 as the significant level. No statistically significant difference was observed between the drug-treated and control groups. To probe the potential liver damage, the levels of liver transaminases were checked in the plasma that reported no significant differences for alanine aminotransferase **(Figure 6a)**, aspartate aminotransferase **(Figure 6b),** and alkaline phosphatase **(Figure 6c)** between the treated and control groups. Similarly, we evaluated the levels of urea in blood samples to assess the potential changes in kidney function. Here, a significant difference was observed for the group treated with RMP-ME, when compared to the control group **(Figure 6d)**. The study on the oral bioavailability of compound **8** displayed an inhibition of *Mtb* growth in mice plasma **(Table 5)**.

Histology of liver **(Figure 7)** and kidneys **(Figure 8)** revealed similar morphology in all the groups, implying that no gross abnormalities were caused by the treatments.

The efficacy of compound **8** was analyzed by infecting the mice with *Mtb* H37Rv strain followed by subjecting the infected animals to the treatment with compound **8** or vehicle. The homogenized lung samples were plated at a dilution of 1:100 to 1:10,000, at which no growth of *Mtb* colonies was observed. Therefore, the homogenized lung samples were re-inoculated on agar plates in undiluted form and at 1:10 dilution; however, again, no colony was observed **(Figure 9)**. Control experiments with vehicles, RPM, and RPM-CE behaved as expected **(Figure 9)**.

Mode of Action Studies

Although the antitubercular activity of the benzofuroxan derivative **8** was originally attributed to its potential to generate and release nitric oxide (NO), we believe this to be no longer the case, since the compound could not release NO in the Griess assay (a chemical test to analyze nitrite ions in a solution, data not shown). An alternative mechanism was proposed as mentioned below.

Microarray analysis of *Mtb* treated with compound **8** or vehicle control revealed a significant up-regulation in the majority of ribosomal genes as well as all genes encoding subunits of the ATP synthase **(Figure 10** and **Supplementary Table S1)**. This included EF-G, which induces GTP-dependent translocation of nascent peptide chains from the A- to the P-site in the ribosome and EF-Tu, which promotes GTP-dependent binding of aminoacylated tRNAs to the A-site in ribosomes. No up-regulation of heat shock proteins was observed, which in fact demonstrated a down-regulation of hsp, htrA, and hspR

(Supplementary Table S1). Similarly, up-regulation of ribosomal proteins was observed upon treatment of *Mtb* with the inhibitors of protein synthesis. Our data indicated an up-regulation of a large number of operons as well as single genes encoding ribosomal proteins, which in turn suggested that compound **8** could affect protein synthesis by inhibiting the ribosome. Boshoff and coworkers (2004)[65] divided the protein synthesis inhibitors into two classes on the basis of their effect on the expression of heat shock proteins (either no effect or up-regulation). Compound **8** did not increase the abundance of transcripts encoding heat shock proteins, and in fact, decreased the levels of three transcripts (*hsp*, *htrA*, and *hspR*). The results of the study on the inhibition of protein synthesis indicated compound **8** to behave more like an inhibitor of initiation of translation, such as tetracyclines, rather than an inhibitor of protein synthesis that leads to mis-translation, such as aminoglycosides. Further studies are required to define the exact MOA of compound **8**, including its binding site and inhibition of the *Mtb* ribosome, ATP synthase, or other targets.

CONCLUSIONS

Twenty-two new N-oxide containing compounds were synthesized followed by *in vitro* and *in vivo* evaluation of their antitubercular activity against *Mtb*. The amide–furoxan series (**4a**–**c**) was observed to be the most promising compounds with MIC_{90} values around 0.40 μM against actively replicating *Mtb* and SI values ranging from 2033.3 to 3204.7. The benzofuroxan series (**8**–**17**) also presented promising antitubercular activity, especially compound **8**, which reported MIC_{90} value of 1.1 and 6.6 μM against actively growing and non-replicating Mtb, respectively. Compound **8** also displayed high activity

in the macrophage model of infection. In addition, *in vivo* studies employing the mouse model of infection demonstrated the sterilizing activity for compound **8**. No detectable *Mtb* was observed in the lungs of mice treated, while control mice displayed expected number of colony forming units (CFUs). Altogether, these findings highlighted the benzofuroxan derivative **8** as a novel lead compound for designing antitubercular drug with sterilizing activity superior to rifampicin in the mouse model of infection.

EXPERIMENTAL SECTION

Chemistry

Melting points (mp) were measured using an electrothermal melting point apparatus (SMP3; Bibby Stuart Scientific) or in a Mettler FP82+FP80 apparatus (Greifense, Switzerland). Infrared spectroscopy (KBr disc) were performed on a FTIR-8300 Shimadzu or a Nicolet Nexu FTIR Thermo® spectrometer, and the frequencies are expressed in cm^{-1}. The NMR for ^{1}H and ^{13}C of all compounds were performed on a Bruker Fourier with Dual probe $^{13}C/^{1}H$ (300-MHz) NMR spectrometer or Bruker 400 Ultrashield^{TM} $^{13}C/^{1}H$ (400-MHz) NMR spectrometer using deuterated chloroform ($CDCl_3$) or dimethyl sulfoxide (DMSO-d_6) as solvent and the chemical shifts were expressed in parts per million (ppm) relative to tetramethylsilane. The signal multiplicities are reported as singlet (s), doublet (d), doublet of doublet (dd), and multiplet (m). Elemental microanalysis (C, H and N) was performed on a Perkin-Elmer model 2400 analyzer or a CHN-900 Elemental Analyzer (LECO, Tres Cantos, Spain) and the data were within ± 0.4% of the theoretical values. HRMS (ESI^{+}) data were acquired using a Bruker Maxis Impact® quadrupole time of flight tandem mass spectrometer (Q-

TOF MS/MS) and the mass spectra values are reported as *m*/*z*. The compounds were purified on a chromatography column with silica gel (60 Å pore size, 35-75-µm particle size) and the following solvents were used as mobile phase: methanol, ethyl acetate, dichloromethane, hexane and petroleum ether in a flow rate of approximately 20 mL/min. The reaction progress of all compounds was monitored by thin-layer chromatography (TLC), which was performed on 2.0- by 6.0-cm^2 aluminum sheets precoated with silica gel 60 (HF-254; Merck) to a thickness of 0.25 mm and revealed under UV light (265 nm). All compounds were analyzed by HPLC, and their purity was confirmed to be greater than 98.5%. HPLC conditions: Shimadzu HPLC model CBM 20-A (Shimadzu®) equipped with UV-VIS detector (model SPD-20A), quaternary pumping system mobile phase (model LC-20AT), solvent degasser (model DGU-20As) and a Agilent® Eclipse XDB C-18 column (250mm x 27 4,6mm; 5µm). For HPLC method it was used an isocratic flow [methanol:water (75:25)]. Reagents and solvents were purchased from commercial suppliers. Compounds **3a-c**,[45–47] **7**,[48] **18**, **19** and **28**[54] were prepared according to previously described methods.

General procedure for the synthesis of compounds 4a-c and 8-17

A solution of compound **3a-c** or **7** (0.87 mmol) in 10 mL of ethanol and 3 drops of glacial acetic acid was stirred at room temperature for 20 min. Next, the appropriate aromatic hydrazide (0.106 g, 0.87 mmol) was added and the mixture was stirred for 12 h. The solvent was concentrated under reduced pressure and ice was added in order to precipitate the desired products. If necessary, the samples could be further purified by silica gel

column chromatography using ethyl acetate-methanol (98:2 v/v) as eluent to give the appropriate compound **4a-c**, and **8-17** with variable yields.

(*E*)-3-carbamoyl-4-((2-((2-isonicotinoylhydrazono)methyl)phenoxy)methyl)-1,2,5-oxadiazole 2-oxide (4a). White powder; yield, 51%; mp, 226 to 229°C. IR V_{max} (cm^{-1}; KBr pellets): 3433 (NH_2 amide), 3203 (N-H), 1669 (C=O amide), 1587 (C=N imine), 1456 (N-O furoxan), 1344 (C-N aromatic), 1145 (C-O ether). ^{1}H NMR (300 MHz, DMSO-d_6, δ ppm) δ: 12.10 (1H; s; N-H), 8.79 (2H; d;), 8.51 (1H; s), 7.91 (1H; dd), 7.84 (2H; d), 7.46 (1H; m), 7.25 (1H, d), 7.11 (1H, t), 5.54 (2H; s) ppm. ^{13}C NMR (75 MHz, DMSO-d_6, δ ppm) δ: 161.55, 156.36, 155.65, 155.24, 150.30, 144.04, 140.47, 131.84, 125.85, 122.59, 121.87, 121.59, 113.36, 110.51 ppm. Anal. Calcd. (%) for $C_{16}H_{12}N_6O_5$: C: 52.18; H: 3.28; N: 22.82. Found: C: 52.25; H: 3.29; N: 22.90. HRMS: *m*/*z* (ESI^+) = 405.0918 $[M + Na]^+$.

(*E*)-3-carbamoyl-4-((3-((2-isonicotinoylhydrazono)methyl)phenoxy)methyl)-1,2,5-oxadiazole 2-oxide (4b). White powder; yield, 59%; mp, 159 to 163°C. IR V_{max} (cm^{-1}; KBr pellets): 3439 (NH_2 amide), 3201 (N-H), 1712 (C=O amide), 1591 (C=N imine), 1485 (N-O furoxan), 1327 (C-N aromatic), 1147 (C-O ether). ^{1}H NMR (300 MHz, DMSO-d_6, δ ppm) δ: 12.09 (1H; s; N-H), 8.78 (2H; d), 8.46 (1H; s), 7.81 (3H; d), 7.41 (3H; m), 5.48 (2H; s) ppm. ^{13}C NMR (75 MHz, DMSO-d_6, δ ppm) δ: 156.96, 150.22, 147.97, 147.44, 142.63, 140.97, 132.70, 127.87, 122.48, 113.82, 113.14, 109.30, 105.24, 102.74 ppm. Anal. Calcd. (%) for $C_{16}H_{12}N_6O_5$: C: 52.18; H: 3.28; N: 22.82. Found: C: 52.27; H: 3.29; N: 22.90. HRMS: *m*/*z* (ESI^+) = 405.0922 $[M + Na]^+$.

(*E*)-3-carbamoyl-4-((4-((2-isonicotinoylhydrazono)methyl)phenoxy)methyl)-1,2,5-oxadiazole 2-oxide (4c). White powder; yield, 67%; mp, 235 to 239°C. IR V_{max} (cm^{-1}; KBr pellets): 3.367 (NH_2 amide), 3255 (N-H), 1708 (C=O amide), 1612 (C=N imine), 1413 (N-O furoxan), 1255 (C-N aromatic), 1122 (C-O ether). ^1H NMR (300 MHz, DMSO-d_6, δ ppm) δ: 11.95 (1H; s; N-H), 8.77 (2H; d;), 8.43 (1H; s), 7.80 (2H; d), 7.71 (2H; d), 7.14 (2H; d), 5.48 (2H; s) ppm. ^{13}C NMR (75 MHz, DMSO-d_6, δ ppm) δ: 162.96, 162.33, 159.91, 156.34, 150.86, 149.52, 141.14, 129.65, 128.08, 122.14, 115.84, 111.05 ppm. Anal. Calcd. (%) for $C_{16}H_{12}N_6O_5$: C: 52.18; H: 3.28; N: 22.82. Found: C: 52.20; H: 3.28; N: 22.84. HRMS: *m*/*z* (ESI^+) = 405.0913 $[M + Na]^+$.

(*E*)-6-((2-isonicotinoylhydrazono)methyl)benzo[c][1,2,5]oxadiazole 1-oxide (8). Yellow powder; yield, 85%; mp, 230 to 232 °C. IR V_{max} (cm^{-1}; KBr pellets): 3324 (N-H), 3045 (NH_2 amide), 1690 (C=O amide), 1600 (C=N imine), 1409 (N-O furoxan), 1273 (C-N aromatic). ^1H NMR (300 MHz, DMSO-d_6, δ ppm) δ: 12.44 (1H; s), 8.80 (2H; d; J = 5.7 Hz), 8.51 (1H; s), 8.03 (3H; m), 7.84 (2H; d; J = 6.0 Hz) ppm. ^{13}C NMR (75 MHz, DMSO-d_6, δ ppm) δ: 162.4, 150.6, 146.6, 140.2, 133.7, 130.8, 130.4, 130.1, 129.4, 121.8, 114.3 ppm. Anal. Calcd. (%) for $C_{13}H_9N_5O_3$: C: 55.13; H: 3.20; N: 24.73. Found: C: 55.22; H: 3.21; N: 24.78. HRMS: *m*/*z* (ESI^+) = 306.0602 $[M + Na]^+$.

(*E*)-6-((2-benzoylhydrazono)methyl)benzo[c][1,2,5]oxadiazole 1-oxide (9). Yellow powder; yield, 80%; mp, 220 to 221 °C. IR V_{max} (cm^{-1}; KBr pellets): 3389 (N-H), 3041 (NH_2 amide), 1641 (C=O amide), 1533 (C=N imine), 1487 (N-O furoxan), 1300 (C-N

aromatic). ^{1}H NMR (300 MHz, DMSO-d_6, δ ppm) δ: 12.24 (1H; s), 8.52 (1H; s), 7.94 (5H; m), 7.58 (3H; m) ppm. ^{13}C NMR (75 MHz, DMSO-d_6, δ ppm) δ: 163.4, 145.0, 132.9, 132.1, 128.5, 127.8, 118.4, 113.5 ppm. Anal. Calcd. (%) for $C_{14}H_{10}N_4O_3$: C: 59.57; H: 3.57; N: 19.85. Found: C: 59.65; H: 3.56; N: 19.88.

(*E*)-6-((2-(4-(tert-butyl)benzoyl)hydrazono)methyl)benzo[c][1,2,5]oxadiazole 1-oxide (10). Yellow powder; yield, 89%; mp, 189 to 191 °C. IR V_{max} (cm^{-1}; KBr pellets): 3341 (N-H), 3068 (NH_2 amide), 1659 (C=O amide), 1532 (C=N imine), 1486 (N-O furoxan), 1287 (C-N aromatic). ^{1}H NMR (300 MHz, DMSO-d_6, δ ppm) δ: 12.16 (1H; s), 8.51 (1H; s), 7.93 (4H; m), 7.56 (3H; d; J = 8.4 Hz), 1.32 (9H; s) ppm. ^{13}C NMR (75 MHz, DMSO-d_6, δ ppm) δ: 160.3, 155.0, 144.7, 130.2, 127.7, 125.3, 118.3, 113.3, 56.0, 34.8, 30.9 ppm. Anal. Calcd. (%) for $C_{18}H_{18}N_4O_3$: C: 63.89; H: 5.36; N: 16.56. Found: C: 63.95; H: 5.37; N: 16.59.

(*E*)-6-((2-(4-nitrobenzoyl)hydrazono)methyl)benzo[c][1,2,5]oxadiazole 1-oxide (11). Yellow powder; yield, 78%; mp, 261 to 262 °C. IR V_{max} (cm^{-1}; KBr pellets): 3373 (N-H), 3073 (NH_2 amide), 1673 (C=O amide), 1525 (C=N imine), 1400 (N-O furoxan), 1357 (C-N aromatic). ^{1}H NMR (300 MHz, DMSO-d_6, δ ppm) δ: 12.50 (1H; s), 8.52 (1H; s), 8.39 (2H; d; J = 8.8 Hz), 8.17 (2H; d; J = 8.8 Hz), 7.95 (3H; m) ppm. ^{13}C NMR (75 MHz, DMSO-d_6, δ ppm) δ: 162.2, 149.4, 146.2, 138.7, 129.4, 123.7 ppm. Anal. Calcd. (%) for $C_{14}H_9N_5O_5$: C: 51.38; H: 2.77; N: 21.40. Found: C: 51.41; H: 2.77; N: 21.42.

(*E*)-6-((2-(2-hydroxybenzoyl)hydrazono)methyl)benzo[c][1,2,5]oxadiazole 1-oxide (12). Yellow powder; yield, 79%; mp, 240 to 241 °C. IR V_{max} (cm^{-1}; KBr pellets): 3573 (O-H), 3332 (N-H), 3100 (NH_2 amide), 1638 (C=O amide), 1532 (C=N imine), 1484 (N-O furoxan), 1341 (C-N aromatic). ^{1}H NMR (300 MHz, DMSO-d_6, δ ppm) δ: 12.12 (1H; s), 11.64 (1H; s), 8.51 (1H; s), 7.95 (4H; m), 7.45 (1H; t; J = 7.5 Hz), 6.99 (2H; m) ppm. ^{13}C NMR (75 MHz, DMSO-d_6, δ ppm) δ: 164.8, 158.7, 145.7, 134.0, 129.0, 119.1, 118.4, 117.3, 116.3, 113.7 ppm. Anal. Calcd. (%) for $C_{14}H_{10}N_4O_4$: C: 56.38; H: 3.38; N: 18.79. Found: C: 56.41; H: 3.37; N: 18.80.

(*E*)-6-((2-(3-hydroxybenzoyl)hydrazono)methyl)benzo[c][1,2,5]oxadiazole 1-oxide (13). Yellow powder; yield, 81%; mp, 265 to 266 °C. IR V_{max} (cm^{-1}; KBr pellets): 3578 (O-H), 3309 (N-H), 3118 (NH_2 amide), 1643 (C=O amide), 1532 (C=N imine), 1371 (N-O furoxan), 1293 (C-N aromatic). ^{1}H NMR (300 MHz, DMSO-d_6, δ ppm) δ: 12.15 (1H; s), 9.80 (1H; s), 8.50 (1H; s), 7.99 (3H; m), 7.33 (3H; m), 7.00 (1H; d; J = 6.9 Hz) ppm. ^{13}C NMR (75 MHz, DMSO-d_6, δ ppm) δ: 163.4, 157.4, 144.9, 134.3, 129.6, 119.0, 118.3, 114.6, 113.3 ppm. Anal. Calcd. (%) for $C_{14}H_{10}N_4O_4$: C: 56.38; H: 3.38; N: 18.79. Found: C: 56.41; H: 3.38; N: 18.82.

(*E*)-6-((2-(4-hydroxybenzoyl)hydrazono)methyl)benzo[c][1,2,5]oxadiazole 1-oxide (14). Yellow powder; yield, 85%; mp, 280 to 281 °C. IR V_{max} (cm^{-1}; KBr pellets): 3573 (O-H), 3332 (N-H), 3096 (NH_2 amide), 1638 (C=O amide), 1523 (C=N imine), 1371 (N-O furoxan), 1280 (C-N aromatic). ^{1}H NMR (300 MHz, DMSO-d_6, δ ppm) δ: 12.02 (1H; s), 10.21 (1H; s), 8.47 (1H; s), 8.01 (2H; m), 7.83 (2H; d; J = 8.7 Hz), 6.87 (3H; d; J = 8.7

Hz) ppm. ^{13}C NMR (75 MHz, DMSO-d_6, δ ppm) δ: 163.0, 161.0, 152.8, 144.0, 136.3, 130.0, 128.8, 123.4, 118.2, 115.1, 114.8 ppm. Anal. Calcd. (%) for $C_{14}H_{10}N_4O_4$: C: 56.38; H: 3.38; N: 18.79. Found: C: 56.39; H: 3.39; N: 18.78.

(*E*)-6-((2-(2-aminobenzoyl)hydrazono)methyl)benzo[c][1,2,5]oxadiazole 1-oxide (15). Yellow powder; yield, 77%; mp, 193 to 194 °C. IR V_{max} (cm^{-1}; KBr pellets): 3501 (NH_2 amine), 3319 (N-H), 3100 (NH_2 amide), 1668 (C=O amide), 1536 (C=N imine), 1477 (N-O furoxan), 1346 (C-N aromatic). ^{1}H NMR (300 MHz, DMSO-d_6, δ ppm) δ: 11.98 (1H; s), 8.44 (1H; s), 7.93 (3H; m), 7.59 (1H; d; *J* = 6.7 Hz), 7.22 (1H; t; *J* = 7.7 Hz), 6.76 (1H; d; *J* = 8.3 Hz), 6.58 (1H; d; *J* = 7.0 Hz), 6.45 (2H; s) ppm. ^{13}C NMR (75 MHz, DMSO-d_6, δ ppm) δ: 165.6, 152.8, 150.3, 143.8, 132.6, 128.5, 118.2, 116.5, 114.6, 112.7 ppm. Anal. Calcd. (%) for $C_{14}H_{11}N_5O_3$: C: 56.57; H: 3.73; N: 23.56. Found: C: 56.64; H: 3.74; N: 23.58.

(*E*)-6-((2-(3-aminobenzoyl)hydrazono)methyl)benzo[c][1,2,5]oxadiazole 1-oxide (16). Yellow powder; yield, 82%; mp, 213 to 215 °C. IR V_{max} (cm^{-1}; KBr pellets): 3501 (NH_2 amine), 3232 (N-H), 3100 (NH_2 amide), 1638 (C=O amide), 1532 (C=N imine), 1416 (N-O furoxan), 1312 (C-N aromatic). ^{1}H NMR (300 MHz, DMSO-d_6, δ ppm) δ: 12.31 (1H; s), 8.86 (1H; s), 8.53 (1H; s), 8.10 (3H; m), 7.87 (3H; s), 7.64 (1H; t; *J* = 7.9 Hz), 7.57 (1H; d; *J* = 7.3 Hz) ppm. ^{13}C NMR (75 MHz, DMSO-d_6, δ ppm) δ: 162.9, 159.6, 150.5, 148.9, 145.2, 134.1, 129.7, 128.9, 126.3, 124.6, 120.7, 114.7 ppm. Anal. Calcd. (%) for $C_{14}H_{11}N_5O_3$: C: 56.57; H: 3.73; N: 23.56. Found: C: 56.59; H: 3.73; N: 23.59.

(*E*)-6-((2-(4-aminobenzoyl)hydrazono)methyl)benzo[c][1,2,5]oxadiazole 1-oxide (17). Yellow powder; yield, 84%; mp, 218 to 200 °C. IR V_{max} (cm^{-1}; KBr pellets): 3478 (NH_2 amine), 3319 (N-H), 3118 (NH_2 amide), 1627 (C=O amide), 1500 (C=N imine), 1380 (N-O furoxan), 1252 (C-N aromatic). ^{1}H NMR (300 MHz, DMSO-d_6, δ ppm) δ: 8.44 (1H; s), 7.92 (3H; m), 7.69 (2H; d; J = 8.6 Hz), 6.60 (2H; d; J = 8.6 Hz), 5.87 (2H; s) ppm. ^{13}C NMR (75 MHz, DMSO-d_6, δ ppm) δ: 165.3, 152.6, 142.9, 129.7, 118.9, 112.6 ppm. Anal. Calcd. (%) for $C_{14}H_{11}N_5O_3$: C: 56.57; H: 3.73; N: 23.56. Found: C: 56.58; H: 3.74; N: 23.57.

General procedure for the synthesis of compounds 20-26

Compound (**18**) (0.3 g; 1.06 mmol) was dissolved in dichloromethane (15 mL) and then cooled by placing it on ice bath. Next, was added the appropriate nitrile (0.15 g; 1.06 mmol) and potassium carbonate (0.18g; 1.32 mmol) in small portions. The reaction mixture was stirred at 40 ºC for 96 hours. After the reaction time, the solvent was evaporated under reduced pressure and the obtained solid was dissolved in 50 mL of ethyl acetate and washed with water. The organic phase was dried with anhydrous magnesium sulfate and the solvent was evaporated giving a yellow solid. The obtained solid was purified by silica gel column chromatography using hexane and ethyl acetate (70:30 v/v) as eluent to give the appropriate compound **20-26** with variable yields.

3-cyano-6-(1,3-dioxolan-2-yl)-2-(p-tolyl)quinoxaline 1,4-dioxide (20). Yellow powder; yield, 9%; mp, 179 to 180 °C. IR V_{max} (cm^{-1}; KBr pellets): 3090 (C-H aromatic), 2233 (CN nitrile), 1328 (N-O), 1073 (C-O ether). ^{1}H NMR (400 MHz, DMSO-d_6, δ ppm) δ:

8.55 (2H; t; *J* = 18.7 Hz), 8.12 (1H; d; *J* = 8.8 Hz), 7.63 (2H; d; *J* = 8.0 Hz), 7.43 (2H; d; *J* = 7.9 Hz), 6.10 (1H; s), 4.09 (4H; m), 2.43 (3H; s) ppm. ^{13}C NMR (75 MHz, DMSO-d_6, δ ppm) δ: 143.1, 143.0, 141.1, 136.7, 132.2, 130.1, 129.2, 129.1, 124.7, 121.0, 117.7, 101.1, 65.3, 21.1 ppm. Anal. Calcd. (%) for $C_{19}H_{15}N_3O_4$: C: 65.32; H: 4.33; N: 12.03. Found: C: 65.36; H: 4.32; N: 12.05.

2-(4-chlorophenyl)-3-cyano-6-(1,3-dioxolan-2-yl)quinoxaline 1,4-dioxide (21). Yellow powder; yield, 13%; mp, 177 to 178 °C. IR V_{max} (cm^{-1}; KBr pellets): 3091 (C-H aromatic), 2235 (CN nitrile), 1330 (N-O), 1093 (C-O ether). ^{1}H NMR (400 MHz, DMSO-d_6, δ ppm) δ: 8.56 (2H; t; *J* = 16.0 Hz), 8.12 (1H; dd; *J* = 26.5 Hz), 7.75 (4H; q; *J* = 25.4 Hz), 6.11 (1H; s), 4.09 (4H; m) ppm. ^{13}C NMR (75 MHz, DMSO-d_6, δ ppm) δ: 144.8, 142.1, 138.8, 137.1, 136.0, 132.1, 130.8, 128.8, 126.5, 121.1, 117.7, 65.3 ppm. Anal. Calcd. (%) for $C_{18}H_{12}ClN_3O_4$: C: 58.47; H: 3.27; N: 11.36. Found: C: 58.67; H: 3.36; N: 11.53.

3-cyano-6-(1,3-dioxolan-2-yl)-2-(4-methoxyphenyl)quinoxaline 1,4-dioxide (22). Yellow powder; yield, 26%; mp, 151 to 152 °C. IR V_{max} (cm^{-1}; KBr pellets): 3085 (C-H aromatic), 2236 (CN nitrile), 1335 (N-O), 1095 (C-O ether). ^{1}H NMR (400 MHz, DMSO-d_6, δ ppm) δ: 8.55 (2H; m), 8.05 (1H; dd), 7.71 (2H; d; *J* = 8.8 Hz), 7.17 (2H; d; *J* = 8.7 Hz), 6.09 (1H; s), 4.08 (4H; m), 3.87 (3H; s) ppm. ^{13}C NMR (75 MHz, DMSO-d_6, δ ppm) δ: 161.2, 144.6, 142.9, 138.8, 132.4, 132.0, 120.6, 119.3, 118.0, 117.7, 113.9, 101.1, 65.2, 55.4 ppm. Anal. Calcd. (%) for $C_{19}H_{15}N_3O_5$: C: 62.46; H: 4.14; N: 11.50. Found: C: 62.51; H: 4.15; N: 11.52.

3-cyano-6-(1,3-dioxolan-2-yl)-2-(4-fluorophenyl)quinoxaline 1,4-dioxide (23). Yellow powder; yield, 30%; mp, 164 to 165 °C. IR V_{max} (cm^{-1}; KBr pellets): 3077 (C-H aromatic), 2234 (CN nitrile), 1330 (N-O), 1097 (C-O ether). ^{1}H NMR (400 MHz, DMSO-d_6, δ ppm) δ: 8.56 (2H; t; *J* = 17.5 Hz), 8.15 (1H; d; *J* = 10.4 Hz), 7.81 (2H; t; *J* = 14.1 Hz), 7.49 (2H; t; *J* = 17.7 Hz), 6.10 (1H; s), 4.09 (4H; m) ppm. ^{13}C NMR (75 MHz, DMSO-d_6, δ ppm) δ: 162.2, 143.2, 142.3, 139.1, 136.7, 133.0, 132.9, 132.3, 124.0, 121.0, 117.7, 115.7, 101.0, 65.3 ppm. Anal. Calcd. (%) for $C_{18}H_{12}FN_3O_4$: C: 61.19; H: 3.42; N: 11.89. Found: C: 61.18; H: 3.41; N: 11.90.

3-cyano-6-(1,3-dioxolan-2-yl)-2-(4-(trifluoromethoxy)phenyl)quinoxaline 1,4-dioxide (24). Yellow powder; yield, 3%; mp, 186 to 187 °C. IR V_{max} (cm^{-1}; KBr pellets): 3077 (C-H aromatic), 2236 (CN nitrile), 1333 (N-O), 1165 (C-O ether). ^{1}H NMR (400 MHz, DMSO-d_6, δ ppm) δ: 8.57 (2H; t; *J* = 15.4 Hz), 8.15 (1H; d; *J* = 8.9 Hz), 7.89 (2H; d; *J* = 8.7 Hz), 7.66 (2H; d; *J* = 8.4 Hz), 6.11 (1H; s), 4.10 (4H; m) ppm. ^{13}C NMR (75 MHz, DMSO-d_6, δ ppm) δ: 149.9, 143.3, 141.9, 139.1, 136.8, 132.7, 132.4, 131.0, 126.7, 121.3, 121.0, 120.9, 117.7, 101.0, 65.3 ppm. Anal. Calcd. (%) for $C_{19}H_{12}F_3N_3O_5$: C: 54.42; H: 2.88; N: 10.02. Found: C: 54.47; H: 2.88; N: 10.06.

3-cyano-6-(1,3-dioxolan-2-yl)-2-(furan-2-yl)quinoxaline 1,4-dioxide (25). Orange powder; yield, 26%; mp, 177 to 179 °C. IR V_{max} (cm^{-1}; KBr pellets): 3087 (C-H aromatic), 2240 (CN nitrile), 1355 (N-O), 1107 (C-O ether). ^{1}H NMR (300 MHz, DMSO-d_6, δ ppm) δ: 8.57 (1H; dd; *J* = 5.2, 3.6 Hz), 8.49 (1H; d; *J* = 8.9 Hz), 8.24 (2H; d;

J = 3.5 Hz), 8.01 (1H; dd; *J* = 8.9, 1.6 Hz), 6.95 (1H; dd; *J* = 3.6, 1.8 Hz), 6.08 (1H; d; *J* = 3.1 Hz), 4.09 (4H; m) ppm. ^{13}C NMR (75 MHz, DMSO-d_6, δ ppm) δ: 146.8, 144.7, 142.3, 140.2, 138.5, 135.6, 133.4, 132.3, 130.0, 120.9, 117.7, 116.8, 113.2, 111.1, 101.2, 65.3 ppm. Anal. Calcd. (%) for $C_{16}H_{11}N_3O_5$: C: 59.08; H: 3.41; N: 12.92. Found: C: 59.12; H: 3.42; N: 12.94.

3-cyano-6-(1,3-dioxolan-2-yl)-2-(thiophen-2-yl)quinoxaline 1,4-dioxide (26). Brown powder; yield, 15%; mp, 171 to 173 °C. IR V_{max} (cm^{-1}; KBr pellets): 3092 (C-H aromatic), 2241 (CN nitrile), 1357 (N-O), 1084 (C-O ether). ^{1}H NMR (300 MHz, DMSO-d_6, δ ppm) δ: 8.60 (1H; dd; *J* = 5.3, 3.6 Hz), 8.51 (1H; d; *J* = 8.8 Hz), 8.45 (1H; dt; *J* = 4.2, 1.2 Hz), 8.13 (1H; dd; *J* = 5.1, 1.0 Hz), 8.03 (1H; dd; *J* = 8.9, 1.7 Hz), 7.43 (1H; dd; *J* = 5.0, 4.2 Hz), 6.09 (1H; d; *J* = 3.8 Hz), 4.09 (4H; m) ppm. ^{13}C NMR (75 MHz, DMSO-d_6, δ ppm) δ: 145.1, 142.5, 138.1, 137.7, 136.8, 135.6, 132.5, 130.2, 127.0, 126.0, 120.7, 117.9, 112.6, 101.2, 65.1 ppm. Anal. Calcd. (%) for $C_{16}H_{11}N_3O_4S$: C: 56.30; H: 3.25; N: 12.31. Found: C: 56.31; H: 3.25; N: 12.30.

REFERENCES

(1) World Health Organization. *Global Tuberculosis Report 2016*; 2016.

(2) World Health Organization. *Global Tuberculosis Report 2013*; 2013.

(3) Rustad, T. R.; Harrell, M. I.; Liao, R.; Sherman, D. R. The Enduring Hypoxic Response of Mycobacterium Tuberculosis. *PLoS One* **2008**, *3* (1), e1502.

(4) Patel, K.; Jhamb, S. S.; Singh, P. P. Models of Latent Tuberculosis: Their Salient Features, Limitations, and Development. *J. Lab. Physicians* **2011**, *3* (2), 75–79.

(5) Zumla, A.; Nahid, P.; Cole, S. T. Advances in the Development of New Tuberculosis Drugs and Treatment Regimens. *Nat. Rev. Drug Discov.* **2013**, *12* (5), 388–404.

(6) Klopper, M.; Warren, R. M.; Hayes, C.; van Pittius, N. C. G.; Streicher, E. M.; Muller, B.; Sirgel, F. A.; Chabula-Nxiweni, M.; Hoosain, E.; Coetzee, G.; van Helden, P. D.; Victor, T. C.; Trollip, A. P. Emergence and Spread of Extensively and Totally Drug-Resistant Tuberculosis, South Africa. *Emerg. Infect. Dis.* **2013**, *19* (3), 449–455.

(7) Slomski, A. South Africa Warns of Emergence of " Totally " Drug-Resistant Tuberculosis. *JAMA J. Am. Med. Assoc.* **2013**, *309* (11), 1097–1098.

(8) World Health Organization. *Multidrug and Extensively Drug-Resistant TB (M/XDR-TB): 2010 Global Report on Surveillance and Response*; 2010.

(9) Zumla, A.; Chakaya, J.; Centis, R.; D'Ambrosio, L.; Mwaba, P.; Bates, M.; Kapata, N.; Nyirenda, T.; Chanda, D.; Mfinanga, S.; Hoelscher, M.; Maeurer, M.; Migliori, G. B. Tuberculosis Treatment and Management—an Update on Treatment Regimens, Trials, New Drugs, and Adjunct Therapies. *Lancet Respir. Med.* **2015**, *3* (3), 220–234.

(10) Ma, Z.; Lienhardt, C.; McIlleron, H.; Nunn, A. J.; Wang, X. Global Tuberculosis Drug Development Pipeline: The Need and the Reality. *Lancet* **2010**, *375* (9731), 2100–2109.

(11) World Health Organization. *Global Tuberculosis Report 2014 (WHO/HTM/TB/2014.08)*; 2014.

(12) Frydenberg, A. R.; Graham, S. M. Toxicity of First-Line Drugs for Treatment of Tuberculosis in Children: Review. *Trop. Med. Int. Heal.* **2009**, *14* (11), 1329–1337.

(13) Tasduq, S. A.; Kaiser, P.; Sharma, S. C.; Johri, R. K. Potentiation of Isoniazid-Induced Liver Toxicity by Rifampicin in a Combinational Therapy of

Antitubercular Drugs (Rifampicin, Isoniazid and Pyrazinamide) in Wistar Rats: A Toxicity Profile Study. *Hepatol. Res.* **2007**, *37* (10), 845–853.

(14) Singh, M.; Sasi, P.; Rai, G.; Gupta, V. H.; Amarapurkar, D.; Wangikar, P. P. Studies on Toxicity of Antitubercular Drugs Namely Isoniazid, Rifampicin, and Pyrazinamide in an in Vitro Model of HepG2 Cell Line. *Med. Chem. Res.* **2011**, *20* (9), 1611–1615.

(15) Yee, D.; Valiquette, C.; Pelletier, M.; Parisien, I.; Rocher, I.; Menzies, D. Incidence of Serious Side Effects from First-Line Antituberculosis Drugs among Patients Treated for Active Tuberculosis. *Am. J. Respir. Crit. Care Med.* **2003**, *167* (11), 1472–1477.

(16) Sahasrabudhe, V.; Zhu, T.; Vaz, A.; Tse, S. Drug Metabolism and Drug Interactions: Potential Application to Antituberculosis Drugs. *J. Infect. Dis.* **2015**, *211*, S107–S114.

(17) Saxena, S.; Samala, G.; Sridevi, J. P.; Devi, P. B.; Yogeeswari, P.; Sriram, D. Design and Development of Novel Mycobacterium Tuberculosis L-Alanine Dehydrogenase Inhibitors. *Eur. J. Med. Chem.* **2015**, *92*, 401–414.

(18) Baldwin, P. R.; Reeves, A. Z.; Powell, K. R.; Napier, R. J.; Swimm, A. I.; Sun, A.; Giesler, K.; Bommarius, B.; Shinnick, T. M.; Snyder, J. P.; Liotta, D. C.; Kalman, D. Monocarbonyl Analogs of Curcumin Inhibit Growth of Antibiotic Sensitive and Resistant Strains of Mycobacterium Tuberculosis. *Eur. J. Med. Chem.* **2015**, *92*, 693–699.

(19) Ng, P. S.; Manjunatha, U. H.; Rao, S. P. S.; Camacho, L. R.; Ma, N. L.; Herve, M.; Noble, C. G.; Goh, A.; Peukert, S.; Diagana, T. T.; Smith, P. W.; Kondreddi, R. R. Structure Activity Relationships of 4-Hydroxy-2-Pyridones: A Novel Class of Antituberculosis Agents. *Eur. J. Med. Chem.* **2015**, *106*, 144–156.

(20) Fernandes, G. F. dos S.; Chin, C. M.; Santos, J. L. Dos. Advances in Drug Discovery of New Antitubercular Multidrug-Resistant Compounds.

Pharmaceuticals **2017**, *10* (2), 51.

(21) Fernandes, G. F. S.; Jornada, D. H.; Souza, P. C.; Man Chin, C.; Pavan, F. R.; Santos, J. L. Current Advances in Antitubercular Drug Discovery: Potent Prototypes and New Targets. *Curr. Med. Chem.* **2015**, *22* (27), 3133–3161.

(22) Wallis, R. S.; Maeurer, M.; Mwaba, P.; Chakaya, J.; Rustomjee, R.; Migliori, G. B.; Marais, B.; Schito, M.; Churchyard, G.; Swaminathan, S.; Hoelscher, M.; Zumla, A. Tuberculosis—advances in Development of New Drugs, Treatment Regimens, Host-Directed Therapies, and Biomarkers. *Lancet Infect. Dis.* **2016**, *16* (4), e34–e46.

(23) Bloemberg, G. V.; Keller, P. M.; Stucki, D.; Trauner, A.; Borrell, S.; Latshang, T.; Coscolla, M.; Rothe, T.; Hömke, R.; Ritter, C.; Feldmann, J.; Schulthess, B.; Gagneux, S.; Böttger, E. C. Acquired Resistance to Bedaquiline and Delamanid in Therapy for Tuberculosis. *N. Engl. J. Med.* **2015**, *373* (20), 1986–1988.

(24) Zhang, S.; Chen, J.; Cui, P.; Shi, W.; Shi, X.; Niu, H.; Chan, D.; Yew, W. W.; Zhang, W.; Zhang, Y. Mycobacterium Tuberculosis Mutations Associated with Reduced Susceptibility to Linezolid. *Antimicrob. Agents Chemother.* **2016**, *60* (4), 2542–2544.

(25) Segala, E.; Sougakoff, W.; Nevejans-Chauffour, A.; Jarlier, V.; Petrella, S. New Mutations in the Mycobacterial ATP Synthase: New Insights into the Binding of the Diarylquinoline TMC207 to the ATP Synthase C-Ring Structure. *Antimicrob. Agents Chemother.* **2012**, *56* (5), 2326–2334.

(26) Fernandes, G. F. .; Souza, P. C.; Marino, L. B.; Chegaev, K.; Gugliemo, S.; Lazzarato, L.; Fruttero, R.; Chung, M. C.; Pavan, F. R.; Santos, J. L. Synthesis and Biological Activity of Furoxan Derivatives against Mycobacterium Tuberculosis. *Eur. J. Med. Chem.* **2016**, *123*, 523–531.

(27) Cerecetto, H.; Porcal, W. Pharmacological Properties of Furoxans and Benzofuroxans: Recent Developments. *Mini-Rev. Med. Chem.* **2005**, *5* (1), 57–71.

(28) Hernández, P.; Rojas, R.; Gilman, R. H.; Sauvain, M.; Lima, L. M.; Barreiro, E. J.; González, M.; Cerecetto, H. Hybrid Furoxanyl N-Acylhydrazone Derivatives as Hits for the Development of Neglected Diseases Drug Candidates. *Eur. J. Med. Chem.* **2013**, *59*, 64–74.

(29) Gasco, A.; Fruttero, R.; Sorba, G.; Di Stilo, A.; Calvino, R. NO Donors: Focus on Furoxan Derivatives. *Pure Appl. Chem.* **2004**, *76* (5), 973–981.

(30) Castro, D.; Boiani, L.; Benitez, D.; Hernandez, P.; Merlino, A.; Gil, C.; Olea-Azar, C.; Gonzalez, M.; Cerecetto, H.; Porcal, W. Anti-Trypanosomatid Benzofuroxans and Deoxygenated Analogues: Synthesis Using Polymer-Supported Triphenylphosphine, Biological Evaluation and Mechanism of Action Studies. *Eur. J. Med. Chem.* **2009**, *44* (12), 5055–5065.

(31) Olea-Azar, C.; Rigol, C.; Mendizabal, F.; Cerecetto, H.; Maio, R. Di; Gonzalez, M.; Porcal, W.; Morello, A.; Repetto, Y.; Maya, J. D. Novel Benzo[1,2-c]1,2,5-Oxadiazole N-Oxide Derivatives as Antichagasic Agents: Chemical and Biological Studies. *Lett. Drug. Des. Discov.* **2005**, *2*, 294–301.

(32) Suter, W.; Rosselet, A.; Knüsel, F. Mode of Action of Quindoxin and Substituted Quinoxaline-Di-N-Oxides on Escherichia Coli. *Antimicrob. Agents Chemother.* **1978**, *13* (5), 770–783.

(33) Ganley, B.; Chowdhury, G.; Bhansali, J.; Daniels, J. S.; Gates, K. S. Redox-Activated, Hypoxia-Selective DNA Cleavage by Quinoxaline 1,4-Di-N-Oxide. *Bioorg. Med. Chem.* **2001**, *9* (9), 2395–2401.

(34) Cheng, G.; Sa, W.; Cao, C.; Guo, L.; Hao, H.; Liu, Z.; Wang, X.; Yuan, Z. Quinoxaline 1,4-Di-N-Oxides: Biological Activities and Mechanisms of Actions. *Front. Pharmacol.* **2016**, *7* (64), 1–21.

(35) Allen, D. M.; Chng, H. H. Disseminated Mycobacterium Flavescens in a Probable Case of Chronic Granulomatous Disease. *J. Infect.* **1993**, *26*, 83–86.

(36) Ohga, S.; Ikeuchi, K.; Kadoya, R.; Okada, K.; Miyazaki, C.; Suita, S.; Ueda, K.

Intrapulmonary Mycobacterium Avium Infection as the First Manifestation of Chronic Granulomatous Disease. *J. Infect.* **1997**, *34* (2), 147–150.

(37) Mestre, O.; Hurtado-Ortiz, R.; Dos Vultos, T.; Namouchi, A.; Cimino, M.; Pimentel, M.; Neyrolles, O.; Gicquel, B. High Throughput Phenotypic Selection of Mycobacterium Tuberculosis Mutants with Impaired Resistance to Reactive Oxygen Species Identifies Genes Important for Intracellular Growth. *PLoS One* **2013**, *8* (1), e53486.

(38) Voskuil, M. I.; Bartek, I. L.; Visconti, K.; Schoolnik, G. K. The Response of Mycobacterium Tuberculosis to Reactive Oxygen and Nitrogen Species. *Front. Microbiol.* **2011**, *2* (May), 1–12.

(39) Behar, S. M.; Martin, C. J.; Booty, M. G.; Nishimura, T.; Zhao, X.; Gan, H.-X.; Divangahi, M.; Remold, H. G. Apoptosis Is an Innate Defense Function of Macrophages against Mycobacterium Tuberculosis. *Mucosal Immunol.* **2011**, *4* (3), 279–287.

(40) Perskvist, N.; Long, M.; Stendahl, O.; Zheng, L. Mycobacterium Tuberculosis Promotes Apoptosis in Human Neutrophils by Activating Caspase-3 and Altering Expression of Bax/Bcl-X. *J. Immunol.* **2002**, *168* (18), 6358–6365.

(41) Herbst, S.; Schaible, U. E.; Schneider, B. E. Interferon Gamma Activated Macrophages Kill Mycobacteria by Nitric Oxide Induced Apoptosis. *PLoS One* **2011**, *6* (5), e19105.

(42) Dharmaraja, A. T.; Alvala, M.; Sriram, D.; Yogeeswari, P.; Chakrapani, H. Design, Synthesis and Evaluation of Small Molecule Reactive Oxygen Species Generators as Selective Mycobacterium Tuberculosis Inhibitors. *Chem. Commun.* **2012**, *48* (83), 10325–10327.

(43) Fang, F. C. Antimicrobial Reactive Oxygen and Nitrogen Species: Concepts and Controversies. *Nat. Rev. Microbiol.* **2004**, *2* (10), 820–832.

(44) Long, R.; Light, B.; Talbot, J. A. Mycobacteriocidal Action of Exogenous Nitric

Oxide. *Antimicrob. Agents Chemother.* **1999**, *43* (2), 403–405.

(45) Di Stilo, A.; Visentin, S.; Cena, C.; Gasco, A. M.; Ermondi, G.; Gasco, A. New 1,4-Dihydropyridines Conjugated to Furoxanyl Moieties, Endowed with Both Nitric Oxide-like and Calcium Channel Antagonist Vasodilator Activities. *J. Med. Chem.* **1998**, *41* (27), 5393–5401.

(46) Maksimovic-Ivanic, D.; Mijatovic, S.; Harhaji, L.; Miljkovic, D.; Dabideen, D.; Fan Cheng, K.; Mangano, K.; Malaponte, G.; Al-Abed, Y.; Libra, M.; Garotta, G.; Nicoletti, F.; Stosic-Grujicic, S. Anticancer Properties of the Novel Nitric Oxide-Donating Compound (S,R)-3-Phenyl-4,5-Dihydro-5-Isoxazole Acetic Acid-Nitric Oxide in Vitro and in Vivo. *Mol. Cancer Ther.* **2008**, *7* (3), 510–520.

(47) Dutra, L. A.; de Almeida, L.; Passalacqua, T. G.; Reis, J. S.; Torres, F. A. E.; Martinez, I.; Peccinini, R. G.; Chin, C. M.; Chegaev, K.; Guglielmo, S.; Fruttero, R.; Graminha, M. A. S.; dos Santos, J. L. Leishmanicidal Activities of Novel Synthetic Furoxan and Benzofuroxan Derivatives. *Antimicrob. Agents Chemother.* **2014**, *58* (8), 4837–4847.

(48) Ghosh, P. B.; Whitehouse, M. W. Potential Antileukemic and Immunosuppressive Drugs. Preparation and in Vitro Pharmacological Activity of Some Benzo-2,1,3-Oxadiazoles (Benzofurazans) and Their N-Oxides (Benzofuroxans). *J. Med. Chem.* **1968**, *11*, 305–311.

(49) Wuts, P. G. M.; Greene, T. W. Protection for the Carbonyl Group. In *Greene's Protective Groups in Organic Synthesis*; Wiley-Interscience: New York, 2006; pp 431–532.

(50) Haddadin, M. J.; Issidorides, C. H. Application of Benzofurazan Oxide to the Synthesis of Heteroaromatic N-Oxides. *Heterocycles* **1976**, *4* (4), 767–816.

(51) Haddadin, M. J.; Issidorides, C. H. Enamines with Isobenzofuroxan: A Novel Synthesis of Quinoxaline-Di-N-Oxides. *Tetrahedron Lett.* **1965**, *6* (36), 3253–3256.

(52) Issidorides, C. H.; Haddadin, M. J. Benzofurazan Oxide. II. Reactions with Enolate Anions. *J. Org. Chem.* **1966**, *31*, 4067–4068.

(53) Zarranz, B.; Jaso, A.; Aldana, I.; Monge, A.; Maurel, S.; Deharo, E.; Jullian, V.; Sauvain, M. Synthesis and Antimalarial Activity of New 3-Arylquinoxaline-2-Carbonitrile Derivatives. *Arzneimittel-Forschung-Drug Res.* **2005**, *55* (12), 754–761.

(54) Fernandes, G. F. dos S.; Moreno-Viguri, E.; Santivañez-Veliz, M.; Paucar, R.; Chin, C. M.; Pérez-Silanes, S.; Santos, J. L. dos. A Comparative Study of Conventional and Microwave-Assisted Synthesis of Quinoxaline 1,4-Di-N-Oxide N-Acylhydrazones Derivatives Designed as Antitubercular Drug Candidates. *J. Heterocycl. Chem.* **2017**, *54* (4), 2380–2388.

(55) Palomino, J.; Martin, A.; Camacho, M.; Guerra, H.; Swings, J.; Portaels, F. Resazurin Microtiter Assay Plate: Simple and Inexpensive Method for Detection of Drug Resistance in Mycobacterium Tuberculosis Resazurin Microtiter Assay Plate : Simple and Inexpensive Method for Detection of Drug Resistance in Mycobacterium Tuberculosis. *Antimicrob. Agents Chemother.* **2002**, *46* (8), 2720–2722.

(56) Pavan, F. R.; Maia, P. I. D. S.; Leite, S. R. a; Deflon, V. M.; Batista, A. a.; Sato, D. N.; Franzblau, S. G.; Leite, C. Q. F. Thiosemicarbazones, Semicarbazones, Dithiocarbazates and Hydrazide/hydrazones: Anti - Mycobacterium Tuberculosis Activity and Cytotoxicity. *Eur. J. Med. Chem.* **2010**, *45* (5), 1898–1905.

(57) Orme, I. Search for New Drugs for Treatment of Tuberculosis. *Antimicrob Agents Chemother* **2001**, *45* (7), 1943–1946.

(58) Cho, S. H.; Warit, S.; Wan, B.; Hwang, C. H.; Pauli, G. F.; Franzblau, S. G. Low-Oxygen-Recovery Assay for High-Throughput Screening of Compounds against Nonreplicating Mycobacterium Tuberculosis. *Antimicrob. Agents Chemother.* **2007**, *51* (4), 1380–1385.

(59) Collins, L. A.; Franzblau, S. G. Microplate Alamar Blue Assay versus BACTEC 460 System for High- Throughput Screening of Compounds against Mycobacterium Tuberculosis and Mycobacterium Avium. *Antimicrob. Agents Chemother.* **1997**, *41* (5), 1004–1009.

(60) Piddington, D. L.; Kashkouli, A.; Buchmeier, N. A. Growth of Mycobacterium Tuberculosis in a Defined Medium Is Very Restricted by Acid pH and Mg2+ Levels. *Infect. Immun.* **2000**, *68* (8), 4518–4522.

(61) Katila, M. L.; Mattila, J.; Brander, E. Enhancement of Growth of Mycobacterium Malmoense by Acidic pH and Pyruvate. *Eur. J. Clin. Microbiol. Infect. Dis.* **1989**, *8* (11), 998–1000.

(62) Artigas, A.; Wernerman, J.; Arroyo, V.; Vincent, J. L.; Levy, M. Role of Albumin in Diseases Associated with Severe Systemic Inflammation: Pathophysiologic and Clinical Evidence in Sepsis and in Decompensated Cirrhosis. *J. Crit. Care* **2016**, *33*, 62–70.

(63) Bertucci, C.; Domenici, E. Reversible and Covalent Binding of Drugs to Human Serum Albumin: Methodological Approaches and Physiological Relevance. *Curr. Med. Chem.* **2002**, *9* (15), 1463–1481.

(64) De Freitas, E. S.; Da Silva, P. B.; Chorilli, M.; Batista, A. A.; De Oliveira Lopes, É.; Da Silva, M. M.; Leite, C. Q. F.; Pavan, F. R. Nanostructured Lipid Systems as a Strategy to Improve the in Vitro Cytotoxicity of ruthenium(II) Compounds. *Molecules* **2014**, *19* (5), 5999–6008.

(65) Boshoff, H. I. M.; Myers, T. G.; Copp, B. R.; McNeil, M. R.; Wilson, M. A.; Barry, C. E. The Transcriptional Responses of Mycobacterium Tuberculosis to Inhibitors of Metabolism. *J. Biol. Chem.* **2004**, *279* (38), 40174–40184.

(66) Snewin, V. A.; Gares, M. P.; Ó Gaora, P.; Hasan, Z.; Brown, I. N.; Young, D. B. Assessment of Immunity to Mycobacterial Infection with Luciferase Reporter Constructs. *Infect. Immun.* **1999**, *67* (9), 4586–4593.

(67) Bapela, N. B.; Lall, N.; Fourie, P. B.; Franzblau, S. G.; Van Rensburg, C. E. J. Activity of 7-Methyljuglone in Combination with Antituberculous Drugs against Mycobacterium Tuberculosis. *Phytomedicine* **2006**, *13* (9–10), 630–635.

(68) Scior, T.; Garcés-Eisele, S. J. Isoniazid Is Not a Lead Compound for Its Pyridyl Ring Derivatives, Isonicotinoyl Amides, Hydrazides, and Hydrazones: A Critical Review. *Curr. Med. Chem.* **2006**, *13* (18), 2205–2219.

(69) Straniero, V.; Pallavicini, M.; Chiodini, G.; Zanotto, C.; Volonte, L.; Radaelli, A.; Bolchi, C.; Fumagalli, L.; Sanguinetti, M.; Menchinelli, G.; Delogu, G.; Battah, B.; Morghen, C. D. G.; Valoti, E. 3-(Benzodioxan-2-Ylmethoxy)-2,6-Difluorobenzamides Bearing Hydrophobic Substituents at the 7-Position of the Benzodioxane Nucleus Potently Inhibit Methicillin-Resistant Sa and Mtb Cell Division. *Eur. J. Med. Chem.* **2016**, *120*, 227–243.

(70) Wube, A. A.; Bucar, F.; Hochfellner, C.; Blunder, M.; Bauer, R.; Hüfner, A. Synthesis of N-Substituted 2-[(1E)-Alkenyl]-4-(1H)-Quinolone Derivatives as Antimycobacterial Agents against Non-Tubercular Mycobacteria. *Eur. J. Med. Chem.* **2011**, *46*, 2091–2101.

(71) Ganihigama, D. U.; Sureram, S.; Sangher, S.; Hongmanee, P.; Aree, T.; Mahidol, C.; Ruchirawat, S.; Kittakoop, P. Antimycobacterial Activity of Natural Products and Synthetic Agents: Pyrrolodiquinolines and Vermelhotin as Anti-Tubercular Leads against Clinical Multidrug Resistant Isolates of Mycobacterium Tuberculosis. *Eur. J. Med. Chem.* **2015**, *89*, 1–12.

(72) Vandal, O. H.; Nathan, C. F.; Ehrt, S. Acid Resistance in Mycobacterium Tuberculosis. *J Bacteriol* **2009**, *191* (15), 4714–4721.

(73) Dutta, N. K.; Karakousis, P. C. Latent Tuberculosis Infection: Myths, Models, and Molecular Mechanisms. *Microbiol Mol Biol Rev* **2014**, *78* (3), 343–371.

(74) OECD. Test No. 117: Partition Coefficient (N-Octanol/water), HPLC Method. In *OECD Guidelines for the Testing of Chemicals*; OECD Publishing: Paris, 2004; pp

1–11.

SUPPORTING INFORMATION

The supporting information contains spectral characterization data, details of the methodology of all biological experiments and microarrays data. The Supporting Information is available free of charge via the Internet at http://pubs.acs.org.

AUTHOR INFORMATION

*These authors contributed equally

Corresponding Authors

#Jean Leandro dos Santos: Phone: +55 16 3301 6972; E-mail: santosjl@fcfar.unesp.br. Fernando Rogério Pavan: Phone: +55 16 3301 4667; E-mail: fernandopavan@fcfar.unesp.br

Notes

The authors declare no competing financial interests.

ACKNOWLEDGMENTS

This study was supported by Fundação de Amparo à Pesquisa do Estado de São Paulo (FAPESP grants 2013/14957-5; 2014/02240-1; 2014/24811-0; 2014/11586-9; 2014/03920-6; 2015/19531-1; 2016/09502-7; 2016/02860-5), Programa de Estágio no Exterior (PROPG-UNESP 2012); Conselho Nacional de Desenvolvimento Científico e

Tecnológico (CNPQ grant: 162676/2013-1), Programa de Apoio ao Desenvolvimento Científico da Faculdade de Ciências Farmacêuticas da UNESP (PADC-FCF UNESP), and the USA National Institute of Allergy and Infections Diseases (preclinical services contract HHSN272201100009l). This work was also supported by the Francis Crick Institute which receives its core funding from Cancer Research UK (FC001060), the UK Medical Research Council (FC001060), and the Wellcome Trust (FC001060). The authors thanks Professor Alberto Gasco for his constribution to the discussion.

ABBREVIATIONS USED

1,8-diazabicyclo[5.4.0]undec-7-ene (DBU); Dichloromethane (DCM); Extensively drug-resistant (XDR); Food and Drug Administration (FDA); Human immunodeficiency virus (HIV); Infrared spectroscopy (IR); Multidrug-resistant (MDR); Minimum bactericidal concentration (MBC); *Mycobacterium tuberculosis* (*Mtb*); Nuclear magnetic resonance (NMR); Quinoxaline 1,4-di-*N*-oxide (QdNO); Reactive oxygen species (ROS); Resazurin microtiter assay (REMA); rifampicin (RMP); Selectivity index (SI); Totally drug-resistant (TDR); Tuberculosis (TB); World Health Organization (WHO).

Scheme 1. Preparation of the compounds of series 1.[a]

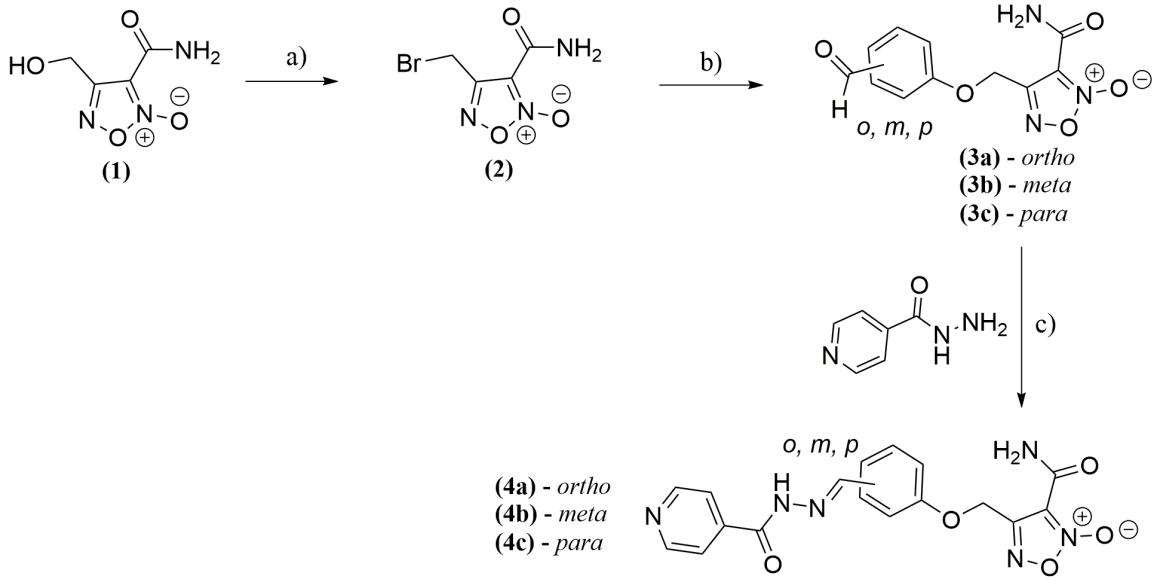

[a]Reagents and conditions: **(a)** thionyl bromide, DMF, r.t., 30 min; **(b)** DBU, 2, 3 or 4-hydroxybenzaldehyde, DCM, r.t., 1 h; **(c)** ethanol, acetic acid, r.t., 12 h.

Scheme 2. Preparation of the compounds of series 2.[a]

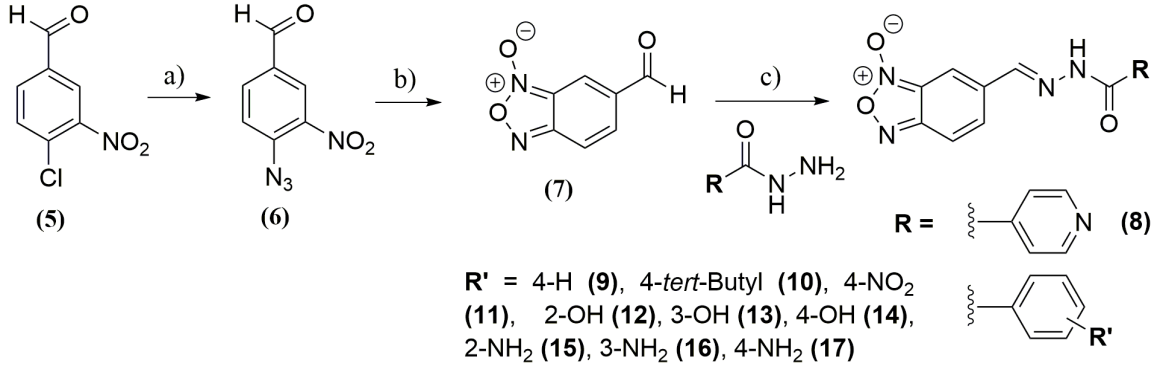

[a]Reagents and conditions: **(a)** NaN_3, DMSO, 75 ºC, 1 h; **(b)** toluene, reflux, 2h; **(c)** aromatic hydrazide, ethanol, acetic acid, r.t., 12 h.

Scheme 3. Preparation of the compounds of series 3.[a]

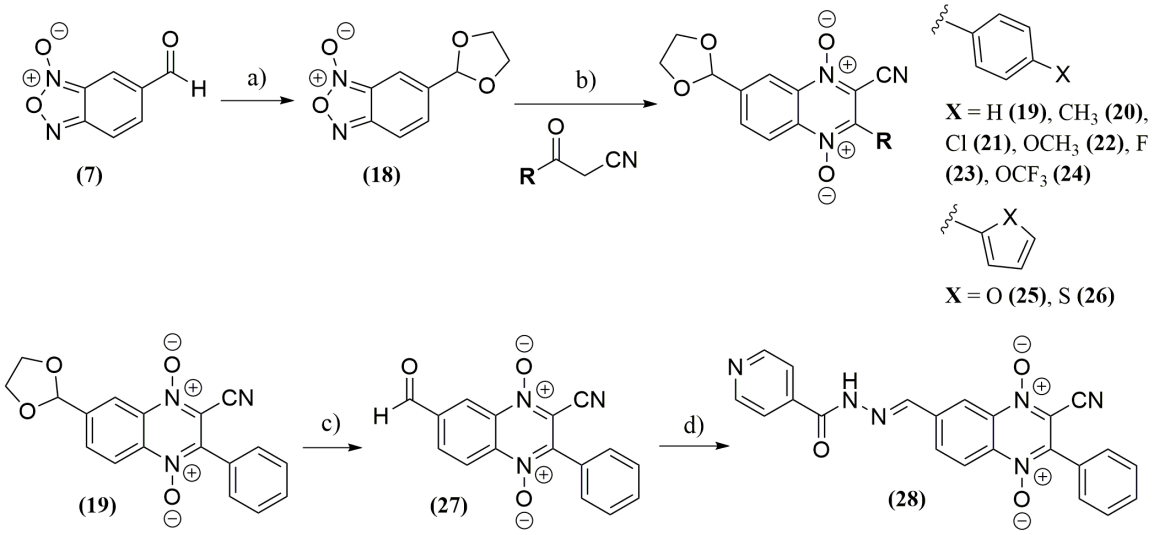

[a]Reagents and conditions: **(a)** toluene, ethylene glycol, *p*-toluenesulfonic acid, reflux, 12 h; **(b)** DCM, K_2CO_3, 40 ºC, 96 h; **(c)** acetone, HCl, r.t., 48 h; **(d)** isonicotinohydrazide, ethanol, acetic acid, r.t., 12 h.

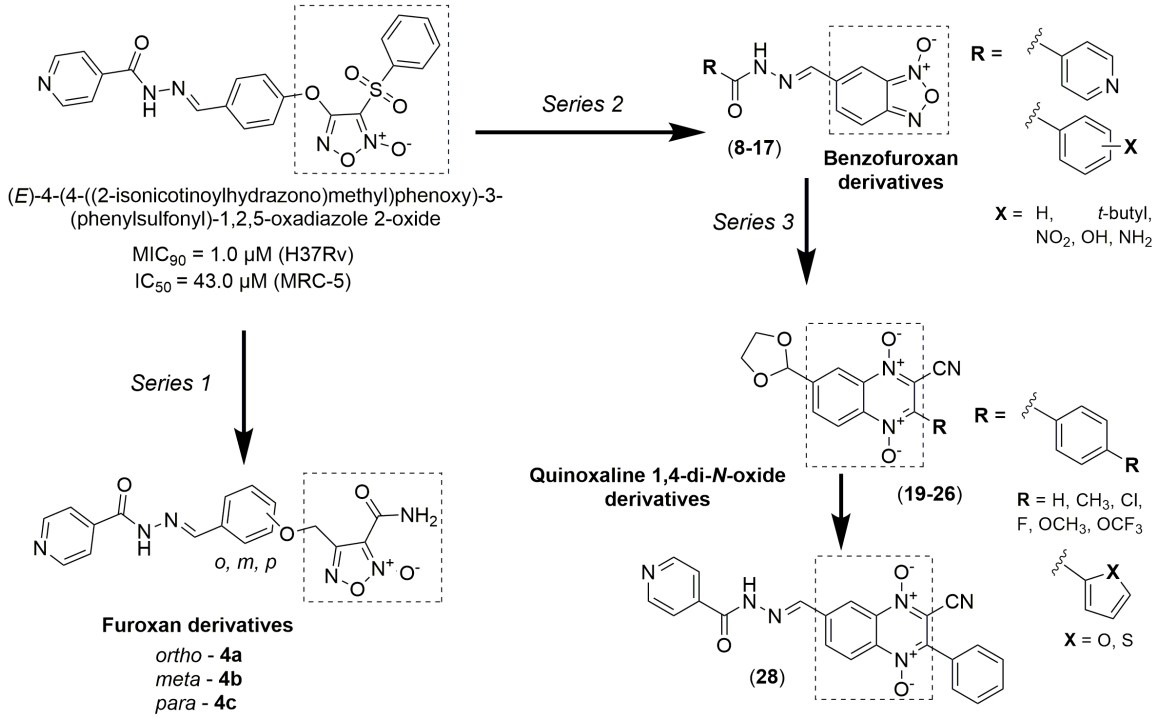

Figure 1. Design of the *N*-oxide containing heterocycles derivatives.

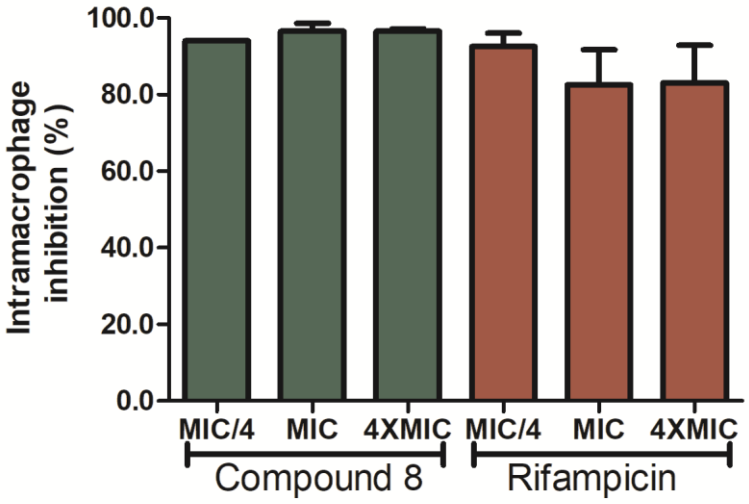

Figure 2. Intramacrophage activity of compound **(8)** and RMP after infection of J774A.1 macrophages with *M. tuberculosis* H37Rv (ATCC 27294). The percentage of inhibition was determined as the mean of three independent assays. The compounds concentrations were: Compound (**8**) 23.86 µg/mL (4xMIC), 5.84 µg/mL (MIC), 1.46 µg/mL (MIC/4); positive control (RMP) 0.064 µg/mL (4xMIC), 0.016 µg/mL (MIC), 0.04 µg/mL (MIC/4). Bars: Means±S.D.

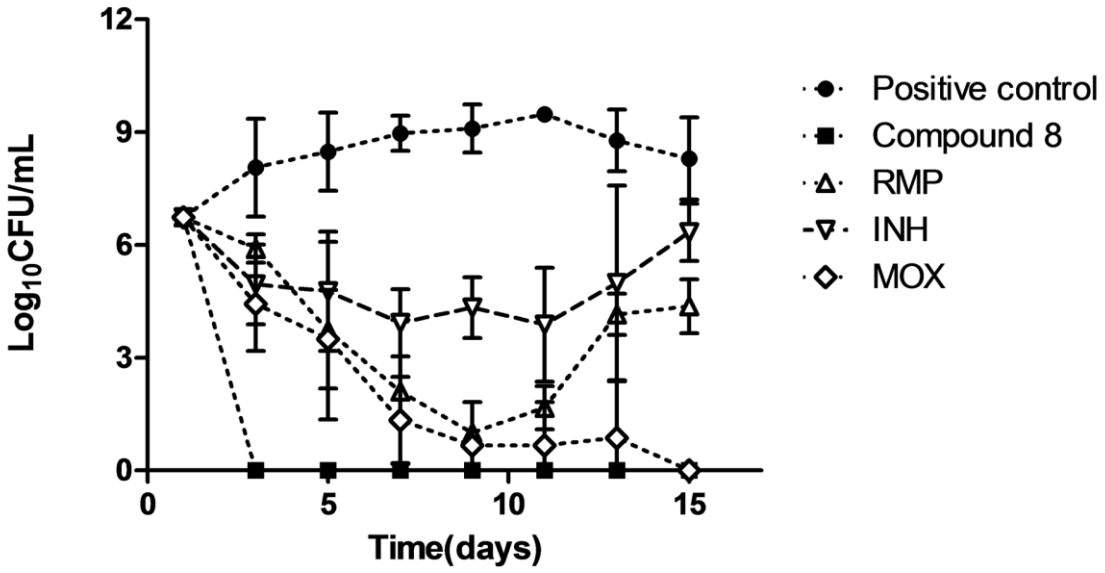

Figure 3. Time-kill curves of the Compound **(8)**, rifampicin, isoniazid and moxifloxacin: results in Log_{10} CFU/mL of the *M. tuberculosis* H37Rv (ATCC 27294) according to time (days). The CFU count was determined as the mean of three independent assays. The compounds concentrations were: 0.72 µM for INH; 0.01 µM for RMP; 0.88 µM for MOX and 41.24 µM for Compound 8. Bars: Mean ± S.D.

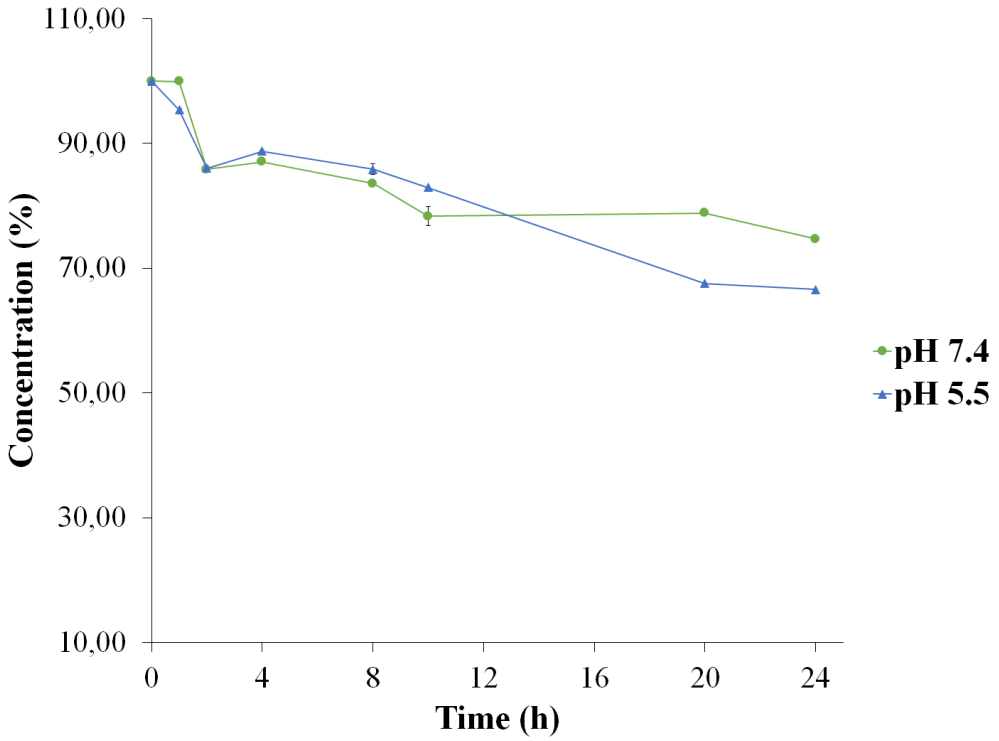

Figure 4. *In vitro* chemical stability. Hydrolytic profile of compound **8** in buffer (pH 5.5 and 7.4) (data are represented as means ± SEMs and expressed as %).

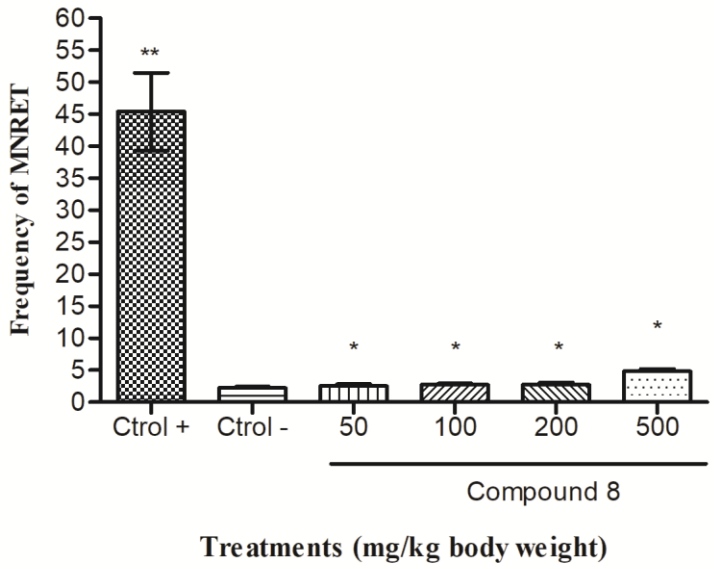

Figure 5. Average frequency of micronucleated reticulocytes (MNRET) and standard deviation of 1000 cells obtained from mice treated with the positive control cyclophosphamide (50 mg/kg), CMC/Tween (negative control), and compound 8 (50, 100, 200, and 500 mg/kg body weight). *$p < 0.05$ (compared to negative control), **$p < 0.05$ (compared to the negative control, and compound 8).

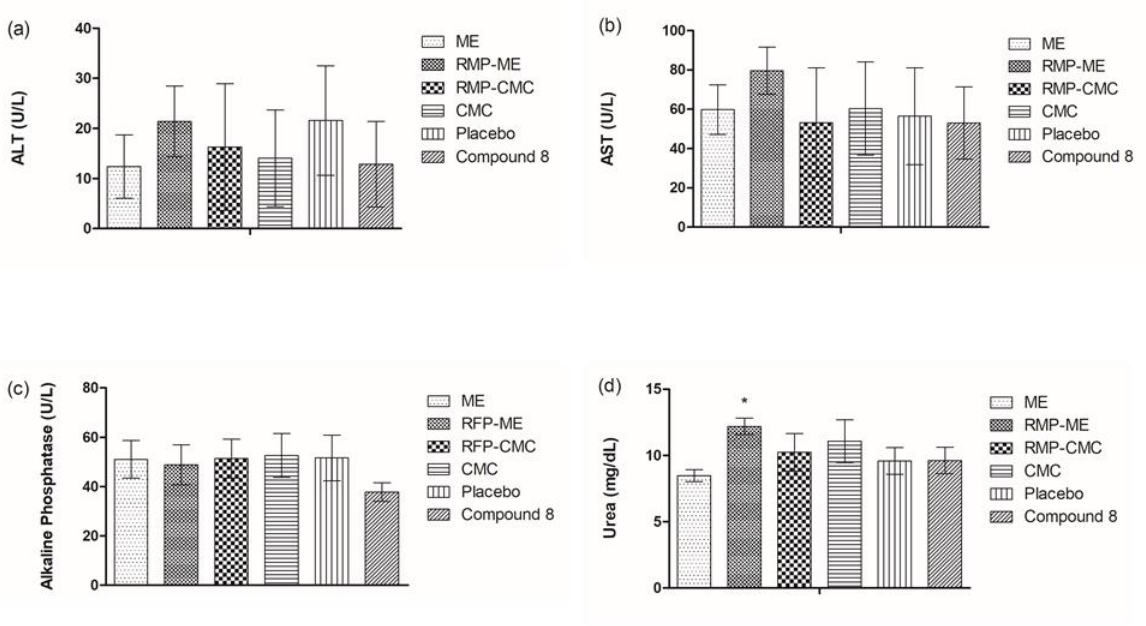

Figure 6. Results of alanine aminotransferase (**6a**), aspartate aminotransferase (**6b**), alkaline phosphatase enzyme activity determination (**6c**) and of urea quantification (**6d**) in the plasma of BALB / c mice. Each compound was administered at a daily oral dose (gavage) at a concentration of 200 mg / kg body weight (n = 4 animals / group) and the RMP at a concentration of 20 mg / kg. The statistical analysis was performed by Graph Pad Prism Version 5.01 software, through Analysis of variance (ANOVA) and Dunnett's test, establishing $P < 0.05$ as significance level. Bars: S.D.

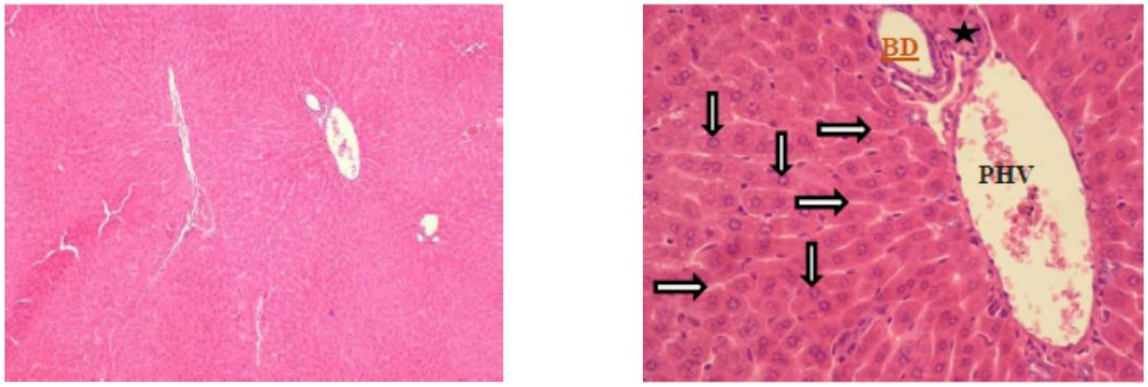

Figure 7. Histological section of liver stained with H / E from the group treated with compound **(8)**. In these groups, histological sections stained with H / E showed, in general, presence of hepatocytes with polyhedral morphology, grouped in strings separated by sinusoids, forming well-defined hepatic lobes. The sinusoids characterized as wall capillaries coated by typical endothelial cells, had some Kupffer cells. In each border of the hepatic lobe, there was the presence of well-organized structures called portal-space, which is characterized mainly by the presence of portal hepatic vein (PHV), arteriole (A) and bile duct (BD). This set was surrounded by a layer of intact and continuous connective tissue, which appeared cut off by channels that discharged blood into the sinusoids, which flow into the central lobular vein.

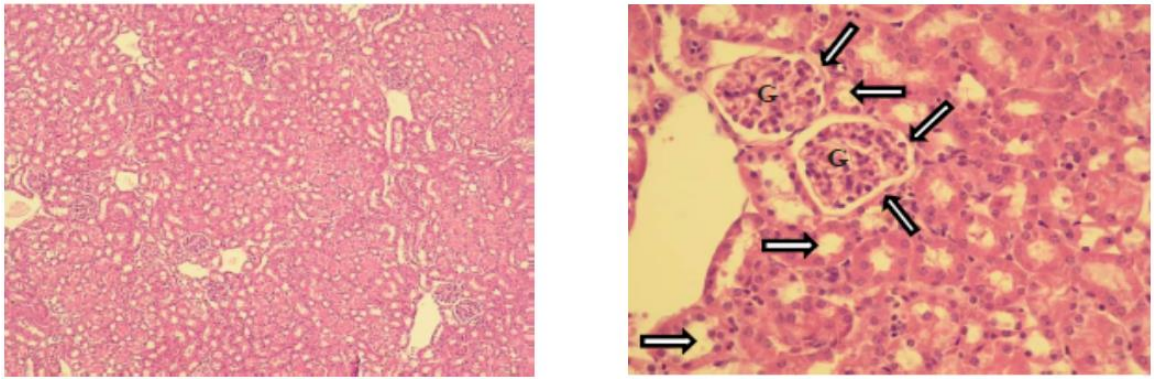

Figure 8. Histological section of kidneys stained with H / E from the group treated with compound (**8)**. Histological sections stained with H / E generally exhibited normal, well established and morphologically normal functional units of the kidney. Each nephron had the Malpighi corpuscle, characterized by the following structures: 1) Bowman's capsule, formed by simple pavement epithelium, and 2) glomerulus (G), characterized by a set of capillaries of fenestrated type. Near the Malpighi corpuscle, it was possible to observe proximal convoluted tubules formed by a simple layer of high cuboidal epithelial cells, which have brush edges facing the light of the tubules. Also adjacent to the Malpighi corpuscles were distal tubules formed by low cuboidal cells.

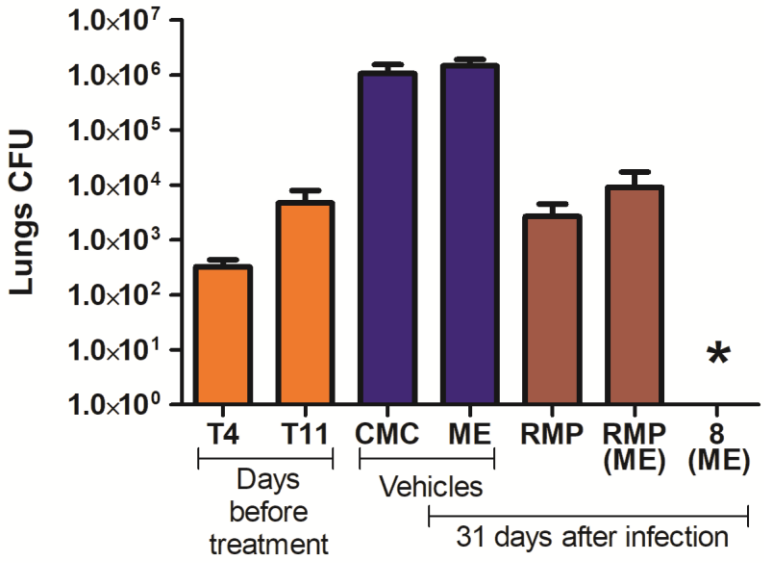

Figure 9. Efficacy of compound **(8)** in microemulsion and controls administrated once daily by oral gavage of a 200 µL suspension. Efficacy of 200 mg/kg of compound (**8**) against acute TB in mice. Female 20g BALB/c mice were infected by aerosol with a low dose ($5x10^6$ CFU/ml) of *M. tuberculosis* Erdman. Start of treatment commenced at 10 days postinfection and terminated at 29 days postinfection. Dosages were obtained by once-daily dosing by oral gavage. Groups of 7 mice were dosed for 5 consecutive days each week. CFU were determined after 3-day washout period at day 31 postinfection. Both lungs were homogenized and diluted in Hanks' balanced salt solution (HBSS)-Tween, and aliquots were plated on Middlebrook 7H11 medium. Bars: S.D. *Sterilize effect.

(a) (b) (c)

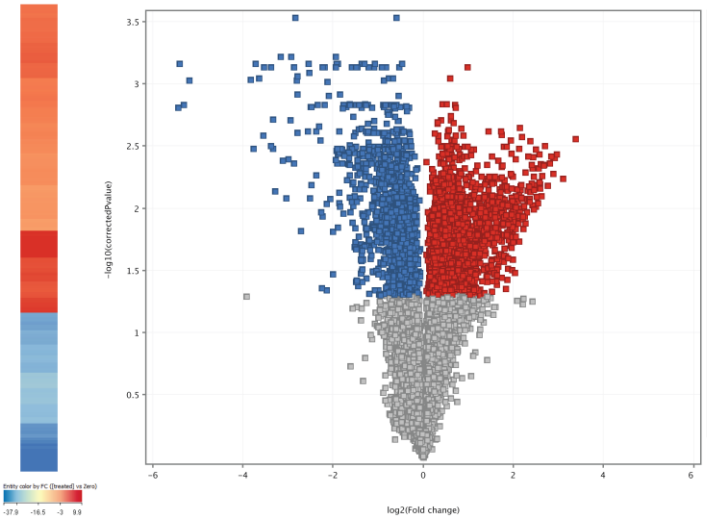

Gene number	Gene name	FC Av (Log_2)	Number of probes detected	Gene number	Gene name	FC Av (Log_2)	Number of probes detected
Rv0053	*rpsF*	1.60	2	Rv1015	*rplY*	1.11	2
Rv0054	*rpsR1*	1.74	1	Rv1630	*rplA*	1.12	1
Rv0055	*rpsI*	1.71	3	Rv1643	*rplT*	1.64	2
Rv0634B	*rpmG2*	1.85	1	Rv2055	*rpsR2*	1.03	1
Rv0640	*rplK*	1.65	2	Rv2057	*rpmG1*	1.50	1
Rv0641	*rplA*	1.33	2	Rv2058	*rpmB2*	1.33	1
Rv0651	*rplJ*	1.30	3	Rv2412	*rpsT*	1.49	2
Rv0652	*rplL*	1.92	2	Rv2441	*rpmA*	1.51	3
Rv0682	*rpsL*	1.92	4	Rv2442	*rplU*	1.77	2
Rv0683	*rpsG*	2.24	3	Rv2785	*rpsO*	1.14	2
Rv0684	*fusA*	2.09	3	Rv2889	*tsf*	1.30	2
Rv0685	*tuf*	2.33	3	Rv2890	*rpsB*	1.68	1
Rv0700	*rpsJ*	2.77	3	Rv2904	*rplS*	1.55	2
Rv0701	*rplC*	2.65	3	Rv2909	*rpsP*	1.51	2
Rv0702	*rplD*	2.18	3	Rv3442	*rpsI*	1.71	2
Rv0703	*rplW*	2.26	3	Rv3443	*rplM*	1.95	3
Rv0704	*rplB*	2.54	2	Rv3456	*rplQ*	1.61	3
Rv0705	*rpsS*	2.86	2	Rv3458	*rpsD*	1.64	3
Rv0706	*rplV*	2.09	3	Rv3459	*rpsK*	1.58	2
Rv0707	*rpsC*	2.28	2	Rv3460	*rpsM*	1.60	3
Rv0708	*rplP*	2.68	1	Rv3461	*rpmJ*	1.70	1
Rv0709	*rpmC*	2.79	2	Rv3924	*rpmH*	1.77	2
Rv0710	*rpsQ*	2.23	3				
Rv0714	*rplN*	1.86	3				
Rv0715	*rplX*	2.12	3	Rv1304	atpB	1.12	1
Rv0716	*rplE*	2.25	2	Rv1305	atpE	1.15	2
Rv0717	*rpsN*	1.33	1	Rv1306	atpF	1.31	1
Rv0718	*rpsZ*	2.30	2	Rv1306/7	atpFH	1.40	2
Rv0718	*rpsH*	2.04	3	Rv1308	atpA	1.77	3
Rv0719	*rplF*	1.95	3	Rv1309	atpG	1.81	2
Rv0720	*rplR*	1.99	2	Rv1310	atpD	1.87	3
Rv0721	*rpsE*	2.34	3	Rv1311	atpC	1.35	2
Rv0722	*rpmD*	2.12	2				
Rv0723	*rplO*	2.03	2				

Figure 10. Genes expression after 4 hours of exposure to compound **(8)** at 2 times of MIC by microarray. (a) Heatmap and (b) Volcano plot, illustrating the effect of compound (**8**) versus vehicle on gene expression in M. tuberculosis H37Rv. (c) Table showing two examples of up-regulated genes associated with the ribosome or ATP synthase.

Table 1. Antitubercular activity of *N*-oxide containing heterocycles against actively replicating and dormant *Mycobacterium tuberculosis* $H_{37}Rv$ (MIC_{90}); cytotoxicity against MRC-5 cell line (IC_{50}); selectivity index (SI) and experimental logP.

Class	Compound	MIC_{90}		Dormant MIC_{90}		Cytotoxicity IC_{50}		SI[a]	LogP[b]
		µg/mL	µM	µg/mL	µM	µg/mL	µM		
Furoxan	**4a**	0.16	0.42	2.95	7.72	326.70	854.00	2033.30	1.3
	4b	0.15	0.40	1.60	4.20	490.10	1281.90	3204.70	1.3
	4c	0.16	0.43	0.78	2.04	443.30	1159.50	2696.50	1.3
Benzofuroxan	**8**	0.31	1.10	-	6.62	147.10	519.20	472.0	1.5
	9	2.40	8.30	-	-	36.80	130.40	15.60	2.2
	10	1.30	3.90	-	-	8.50	25.20	6.30	3.8
	11	1.73	5.29	-	-	-	-	-	0.9
	12	16.40	> 62.0	-	-	-	-	-	1.3
	13	> 25.0	> 62.0	-	-	-	-	-	1.2
	14	> 25.0	> 62.0	-	-	-	-	-	1.2
	15	3.70	12.30	-	-	36.40	122.40	9.90	2.0
	16	5.30	17.80	-	-	24.40	82.10	4.60	1.4
	17	3.16	10.66	>10.0	>10.0	250.0	841.0	78.90	1.2
Quinoxaline	**19**	10.30	30.80	-	-	10.70	31.90	0.90	0.7
	20	5.70	16.50	-	-	6.20	17.20	1.10	1.6
	21	6.40	16.20	-	-	5.00	12.60	0.80	1.8
	22	4.40	12.00	-	-	5.50	15.00	1.20	1.4
	23	8.60	24.30	-	-	7.70	21.80	0.90	1.3
	24	6.50	15.40	-	-	28.00	66.80	4.30	2.2
	25	1.70	5.20	-	-	11.60	35.70	6.80	2.0
	26	4.10	12.10	-	-	5.90	17.30	1.40	1.9
	28	16.30	39.70	-	-	8.60	21.00	0.50	1.0
Standard Drugs	Isoniazid	0.014	0.1	-	1.108.4	-	-	-	-
	Rifampicin	0.082	0.1	-	0.1	N.D.	N.D.	N.D.	N.D.

[a]Abbreviations: SI, ratio between IC_{50} for MRC-5 and MIC_{90}; dash (-) means not determined. [b] Determined by partition coefficient (*n*-octanol/water), HPLC method [74].

Table 2. Results of MIC (µM) determinations with compound **8** against *M. tuberculosis* H37Rv (ATCC 27294) in three different conditions.

Compound	Normal[a]		Acid pH[b]		FBS[c]		BSA[d]	
	MIC (µM)	S.D	MIC (µM)	S.D	MIC (µM)	S.D	MIC (µM)	S.D
8	5.47	1.01	3.41	1.52	11.79	0.93	9.81	1.21
Rifampicin	0.05	0.03	0.02	0.02	0.10	0.08	0.10	0.03

[a]Normal: normal pH media= 6.8. [b]Acid pH: adjusted pH media for 6.0. [c]BFS: 10% bovine fetal serum. [d]*BSA: 4%* bovine serum albumin

Table 3. Antitubercular activity of *N*-oxide containing heterocycles against *Mycobacterium tuberculosis* monoresistant strains

Class	Compound	INHr[a]	RMPr[a]	MOXr[a]	BDQr[a]	CAPr[a]	SMr[a]
		MIC (µM)					
Furoxan	**4a**	>261.71	0.44	0.81	0.81	>261.71	27.4
	4b	>261.71	2.31	1.22	2.56	>261.71	>261.71
	4c	>261.71	1.99	0.66	6.38	>261.71	>261.71
Benzofuroxan	**8**	8.59	3.78	5.72	1.20	15.25	16.98
Standard Drugs	RIF	0.01	>1.00	0.10	0.04	0.21	0.03
	INH	>5.0	0.35	0.28	0.23	>5.00	>5.00
	MOX	0.23	0.12	>8.00	0.26	0.35	0.36
	BDQ	0.01	0.01	0.06	1.70	0.06	0.06
	CAP	-	-	-	-	60.46	1.72
	SM	-	-	-	-	2.55	>100

[a] Abreviations: (INHr) isoniazid resistant; (RMPr) rifampicin resistant; (MOXr) moxifloxacin resistant; (BDQr) Bedaquiline resistant; (CAPr) capreomycin resistant and (SMr) streptomycin resistant. Dash (-) means not determined.

Table 4. In vitro ADMT data for compound 8

Assay	Compound 8
Human plasma protein binding (% free)	46.5
Caco-2 permeability	
A−B P_{app}[a] (cm/s)	5.67 x 10^{-6}
B−A P_{app}[a] (cm/s)	3.90 x 10^{-6}
CYP inhibition IC_{50} (μM)	
CYP2B6	> 20
CYP2C8	> 20
CYP2C19	15.3
CYP3A4	> 20
HepG2 IC_{50} (μM)	16

[a] P_{app} is the apparent permeability rate coefficient.

Table 5. Plasma levels of compound (**8)** (300 mg/kg dose), RMP-ME and RMP-CMC (dose of 20 mg/kg) following a single administration through oral route at times: 0,3h; 1h; 2h and 4h. Experiments were carried out in BALB/c mice.

Compound	**Standard**[a]	**Drug Dose**	**Mice Data**[b]							
			0,3 h		1 h		2 h		4 h	
	MIC (µg/mL) predetermined	(mg/kg/body)	Inhibition (%)	Estimate (µg/mL)	Inhibition (%)	Estimate (µg/mL)	Inhibition (%)	Estimate (µg/mL)	Inhibition (%)	Estimate (µg/mL)
Compound (**8**)-ME	5.84	300	65.67	42.61	79.00	51.26	76.00	49.31	51.33	33.30
RMP-ME	0.015	20	66.33	0.11	63.00	0.31	76.33	0.37	91.00	0.15
RMP-CMC	0.015	20	73.67	0.11	84.00	0.14	62.27	0.10	68.00	0.11

[a]Predetermined by *Resazurin Microtiter Assay (REMA) in vitro*. [b] Determined using plasma mice by *REMA in vitro*, estimative in plasma.

TABLE OF CONTENTS GRAPHIC